

Accepted Manuscript

Synthesis, cytotoxicity and antiviral evaluation of new series of imidazo[4,5-g]quinoline and pyrido[2,3-g]quinoxalinone derivatives

Irene Briguglio, Roberta Loddo, Erik Laurini, Maurizio Fermeglia, Sandra Piras, Paola Corona, Paolo Giunchedi, Elisabetta Gavini, Giuseppina Sanna, Gabriele Giliberti, Cristina Ibba, Pamela Farci, Paolo La Colla, Sabrina Pricl, Antonio Carta

PII: S0223-5234(15)30284-1

DOI: [10.1016/j.ejmech.2015.10.002](https://doi.org/10.1016/j.ejmech.2015.10.002)

Reference: EJMECH 8137

To appear in: *European Journal of Medicinal Chemistry*

Received Date: 7 July 2014

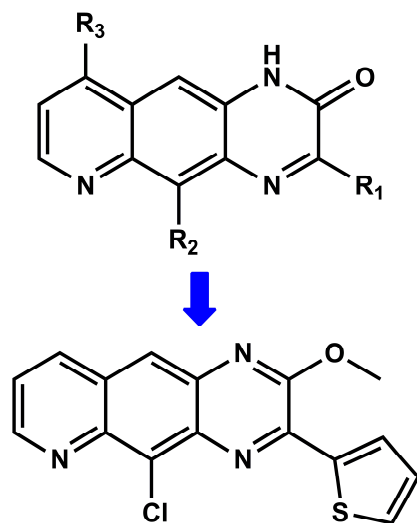
Revised Date: 1 October 2015

Accepted Date: 3 October 2015

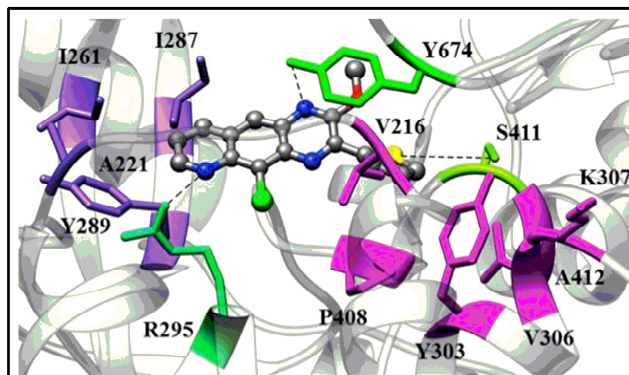
Please cite this article as: I. Briguglio, R. Loddo, E. Laurini, M. Fermeglia, S. Piras, P. Corona, P. Giunchedi, E. Gavini, G. Sanna, G. Giliberti, C. Ibba, P. Farci, P. La Colla, S. Pricl, A. Carta, Synthesis, cytotoxicity and antiviral evaluation of new series of imidazo[4,5-g]quinoline and pyrido[2,3-g]quinoxalinone derivatives, *European Journal of Medicinal Chemistry* (2015), doi: 10.1016/j.ejmech.2015.10.002.

This is a PDF file of an unedited manuscript that has been accepted for publication. As a service to our customers we are providing this early version of the manuscript. The manuscript will undergo copyediting, typesetting, and review of the resulting proof before it is published in its final form. Please note that during the production process errors may be discovered which could affect the content, and all legal disclaimers that apply to the journal pertain.





Compound 21
 $CC_{50} > 100 \mu\text{M}$
 EC_{50} on BVDV = $1.3 \mu\text{M}$



Details of Compound 21 in the BVDV RdRp binding pocket

ACCEPTED MANUSCRIPT

Synthesis, cytotoxicity and antiviral evaluation of new series of imidazo[4,5-g]quinoline and pyrido[2,3-g]quinoxalinone derivatives

Irene Briguglio^{a§}, Roberta Loddo^{b*§}, Erik Laurini^{c§}, Maurizio Fermeglia^c, Sandra Piras^a, Paola Corona^a, Paolo Giunchedi^a, Elisabetta Gavini^a, Giuseppina Sanna^b, Gabriele Giliberti^b, Cristina Ibba^b, Pamela Farci^b, Paolo La Colla^{b+}, Sabrina Pricl^{cd+}, Antonio Carta^{a*+}

^a*Dipartimento di Chimica e Farmacia, Università degli Studi di Sassari, Via Muroni 23/A, 07100 Sassari, Italy*

^b*Dipartimento di Scienze Biomediche, Sezione di Microbiologia e Virologia, Università degli Studi di Cagliari, Cittadella Universitaria s.p.8, Km 0,700, 09042 Monserrato (Ca), Italy*

^c*Molecular Simulation Engineering (MOSE) Laboratory, Department of Engineering and Architecture (DEA), University of Trieste, 34127 Trieste, Italy*

^d*National Interuniversity Consortium for Material Science and Technology (INSTM), Research Unit MOSE-DEA, University of Trieste, 34127 Trieste, Italy*

[§]These authors contributed equally to this work

⁺Senior co-authors

Keywords: imidazo[4,5-g]quinolines, pyrido[2,3-g]quinoxalines, antiviral activity, RNA viruses, DNA viruses.

*Corresponding Authors:

Tel.: +39 079 228722; fax: +39 079 228720. E.mail address acarta@uniss.it;

Tel.: +39 070 6754202; fax: +39 070 6754210. E.mail address rloddo@unica.it

Abstract

Linear aromatic *N*-tricyclic compounds with promising antiviral activity and minimal cytotoxicity were prepared and analyzed in the last years. Specifically, the pyrido[2,3-g]quinoxalinone nucleus was found endowed with high potency against several pathogenic RNA viruses as etiological agents of important veterinary and human pathologies. Following our research program on new antiviral agents we have designed, synthesized and assayed new series of imidazo[4,5-g]quinoline and pyrido[2,3-g]quinoxalinone derivatives. Lead compounds **1-4** were further modified to enhance their antiviral activity and reduce their cytotoxicity. Thus, different substituents were introduced on N atom at position 1 or the O atom at position 2 of the leads; contextually, several groups were inserted on the nitrogen atom at position 7 of diaminoquinoline intermediates. Title compounds were tested in cell-based assays for cytotoxicity and antiviral activity against RNA virus families containing single-stranded (either positive-sense (ssRNA+) or negative-sense (ssRNA-)), and double-stranded genomes (dsRNA), and against two representatives of DNA virus families. Some

derivatives emerged as potential leads for further development as antiviral agents against some viruses of public health significance, such as RSV, Reo, BVDV and HCV. Particularly, compounds **4**, **11b**, **11c**, **13c**, **15a**, **18** and **21** resulted active against BVDV at concentrations ranging from 1.3 to 5 μM . Compound **21** was also evaluated for its activity on the BVDV RdRp. Compound **4** was also tested as potential anti-HCV compound in a subgenomic replication assay. Molecular simulation results provided a molecular rationale for the anti-BVDV activity of these compounds.

1. Introduction

Over 200 species of DNA and RNA viruses are known to be able to infect and cause significant diseases in humans [1, 2]. Examples of DNA pathogen viruses are *Herpesviruses*, e.g., *Herpes simplex virus* type 1 (HSV-1) and *Poxviruses* [3], which can infect both vertebrate and invertebrate animals, or, from *Orthopoxvirus* genus the *Vaccinia virus* (VV). The latter emerged in recent years for its potential use as an attractive bioterrorist weapon [4]. This menace to public health increased our awareness around human vulnerability to this infection, especially since smallpox vaccination was discontinued in 1980 [5-9]. RNA viruses include many highly pathogens affecting humans, several of them showing the ability to cross the species barrier and resulting in zoonotic-human epidemics [10]. Examples of RNA pathogen viruses are *Flaviviruses*, which can cause life-threatening diseases in both humans and animals. This virus family includes three genera: *Pestiviruses*, *Flaviviruses* and *Hepaciviruses*. The *Pestivirus* genus includes animal pathogens of major economic impact for the livestock industry, such as the *Bovine viral diarrhea virus* (BVDV). *Hepatitis C virus* (HCV) is the sole representative of the *Hepacivirus* genus and constitutes the major cause of human hepatitis *per se* [11]. Other important RNA viruses belong to the *Picornaviridae* family. These viruses induce a variety of maladies including meningitis, cold, heart infection, conjunctivitis, and hepatitis. This family includes nine genera, some of which comprise major human pathogens (e.g., *Poliovirus* and *Coxsackievirus*) [12]. At present, no specific antiviral therapy is available for the treatment of *Picornaviridae* infections.

In this scenario, there is an urgent need for new lead compounds that either target distinct stages of the viral replication cycle in a virus-specific way, have a broader spectrum of activity or act through novel mechanisms of action. In this context, according to a long-lasting antiviral research program our group designed and synthesized three new classes of linear aromatic *N*-tricyclic compounds endowed with promising antiviral activity and selectivity index against several pathogenic RNA viruses: triazolo[4,5-*g*]quinolines, imidazo[4,5-*g*]quinolones, and pyrido[2,3-*g*]quinoxalines [13]. All three molecular classes share the same key intermediate: a 6,7-diaminoquinoline scaffold

variously substituted on the nitrogen at position 7. Specifically, the pyrido[2,3-*g*]quinoxalinone nucleus was found particularly active against the *Pestivirus* BVDV and partly against the *Human respiratory syncytial virus* (RSV). Both these two viruses are of major interest for livestock and human therapies, respectively. In antiviral drug discovery, BVDV is commonly used as a surrogate model for *Hepatitis C virus* [14]. Thus, given their interesting activity against BVDV, the pyrido[2,3-*g*]quinoxalinones were also tested against HCV in a subgenomic replication assay that allows viral replication in a human hepatoma cell line (GS4.1). Furthermore, the lead compounds of that series were evaluated in enzyme assays performed with the recombinant BVDV and HCV RNA-dependent RNA polymerases (RdRps) [13]. Unfortunately, both the pyrido[2,3-*g*]quinoxalines and pyrido[2,3-*g*]quinoxalinones resulted more active against the BVDV than the HCV enzyme. Moreover, they showed slight cytotoxicity against several cell lines.

In the light of these results, and with the aim of enhancing the antiviral activity and reducing the cytotoxicity of these molecules, in this work we selected lead compounds **1** and **2** from the previous molecular series (**Fig. 1**), which bear a phenyl and a benzyl substituent at position 3 of the pyrazinone moiety, respectively, for further development. Furthermore, we adopted derivative **3**, which contains an isopropyl side chain at the same position and is totally devoid of activity on all tested viruses and cell lines, as a negative benchmark. Finally, as shown in **Scheme 1**, we synthesized and assayed the thienyl derivative **4** since no derivative bearing a heterocycle moiety at position 3 was previously reported and its intermediate **4b** is readily available on the market.

This study is divided in three parts. In the first part we modified the structure of lead compound **1** by inserting a propyl, cyclohexyl or methylcyclohexyl group on the nitrogen at position 7 of the diaminoquinoline intermediates **8a-c**, as reported in **Scheme 2**.

Unexpectedly, the subsequent cyclization reaction with 2-oxo-2-phenylacetic acid provided, in addition to the desired pyrido[2,3-*g*]quinoxalinone derivatives with the phenyl ring at position 2 (**11a-c**), the imidazo[4,5-*g*]quinolines **9a,b**. Interestingly, the same molecular scaffold was obtained in the past by another chemical route [13]. To verify the reproducibility of this mechanism the diaminoquinolines **8b,c** were submitted to cyclization reaction with 2-oxo-2-(thiophen-2-yl) acetic and 2-oxo-3-phenylpropanoic acids, respectively. In the first case both the pyrido[2,3-*g*]quinoxalinone bearing the thiophene ring at position 2 (**12b**) and the corresponding imidazo[4,5-*g*]quinoline **10b** were obtained. In the second case the reaction afforded the pyrido[2,3-*g*]quinoxalinone **13c** and only non-isolable traces of the corresponding imidazo[4,5-*g*]quinoline **9c**.

In the second part of this study we introduced several substituents - methyl, ethyl, acetonitrile, benzyl and 4-nitrobenzyl group - either on the nitrogen atom at position 1 or on the oxygen atom at position 2, as shown in **Scheme 3**. Through direct alkylation of compound **1**, N-alkyl derivatives (**14a-e**) were always obtained, while the isomeric O-derivatives were not always obtained.

Antiviral evaluation of the N and O alkyl derivatives **14** and **15** highlighted N-methyl (**14a**) and O-methyl (**15a**) derivatives as the only compounds endowed of antiviral activity against BVDV, with EC₅₀ values for compound **15a** comparable to that of lead compound **1**. Moreover, these compounds showed activity also against CVB-5 and Sb-1 (**14a**), RSV and Reo-1 (**15a**) viruses.

Consequently, we submitted the other three lead compounds (**2**, **3** and **4**) only to a methylation reaction to dissect the relevance of the different substituents at position 3, as shown in **Scheme 4**.

All synthesized compounds were tested for cytotoxicity and for activity in cell-based assays against ssRNA⁺ viruses [*Human immunodeficiency virus* (HIV-1), *Coxsackie virus* type B5 (CVB-5), *Polio virus* (Sb-1), *Yellow Fever virus* (YFV), *Bovine Viral Diarrhea virus* (BVDV)], ssRNA⁻ viruses [*Human respiratory syncytial virus* (RSV), *Vesicular stomatitis virus* (VSV)], dsRNA viruses [*Reovirus* (Reo-1)], and DNA viruses [(*Herpes simplex virus* type 1 (HSV-1), *Vaccinia virus* (VV)], with the aim of comparing their antiviral activity with that of the former molecular series. In addition, compound **4** was submitted to the HCV subgenomic replication assay to assess the activity of this new lead compound against this critical human pathogen. Finally, a molecular-base rationale for the anti-BVDV activity of these compounds is proposed based on the results of computer-based simulations.

All viruses selected were among those most harmful to human health. With the exception of YFV, there is no vaccine available against the above-mentioned Flaviviruses to date, and only a few new drugs are currently under successful pre-clinical development in this field [12, 15-19]. This perspective indeed emphasizes the compelling need for the identification of new molecules with therapeutic potential against RNA viruses.

2. Results and discussion

2.1 Chemistry

The synthetic route to obtain compound **4** is illustrated in **Scheme 1**. The key intermediate 8-chloroquinoline-6,7-diamine **4a**, obtained as reported in [20], was submitted to cyclization reaction with 2-oxo-2-(thiophen-2-yl)acetic acid (**4b**) in 10% sulfuric acid to give the expected 5-chloro-3-(thiophen-2-yl)pyrido[2,3-g]quinoxalin-2(1H)-one (**4**) (yield 43%) but not the 2-thiophen-2-yl

isomer (**4c**). As shown in **Scheme 1** and previously reported in [21], the reaction conditions determine its regioselectivity. In fact, the simultaneous presence of the acidic environment and an electron-withdrawing group on the α -carbonyl of **4b** leads to the exclusive formation of the desired isomer **4**.

The diamine intermediates **8a-c**, crucial for the preparation of quinoxalines **11a-c**, **12b** and **13c**, were generally obtained in good yield through nucleophilic substitution of the chlorine at position 7 of the known 7,8-dichloro-6-nitroquinoline (**5**) [22] with the amines **6a-c**. The nitro derivatives intermediates (**7a-c**) were subsequently submitted to reduction reaction with 10% Pd/C in ethanol, as depicted in **Scheme 2**.

The succeeding condensation reaction of the diamines **8a-c** with the appropriate α -ketoacids in refluxed ethanol led not only to the expected pyrido[2,3-*g*]quinoxalinones (**11a-c**, **12b** and **13c**), but also to the imidazo[4,5-*g*]quinolines derivatives **9a-c** and **10b**. This behavior is somewhat different from that previously discussed for compound **4**. In fact, the lack of an acidic environment and the presence of an alkyl group on the nitrogen at position 7 of the diaminoquinolines **8a-c** - which increase the steric hindrance around that site - both reverse the reactivity providing only the 2-aryl isomers **11a-c**, **12b** and **13c**. On the other hand, this reaction is in competition with the formation of the imidazo[4,5-*g*]quinoline nucleus, as previously reported by our group [21].

Scheme 3 reports the synthesis of the pyrido[2,3-*g*]quinoxalinones **14a-e** and pyrido[2,3-*g*]quinoxalines **15a,b,e**. The lead compound **1** was subjected to alkylation reaction with methyl and ethyl sulfate, acetonitrile, benzyl bromide and 4-nitrobenzyl chloride in dimethylformamide (DMF) and Cs_2CO_3 at 60 °C for 1-16 hours. From these reactions the expected N alkyl derivatives (**14a-e**) were isolated, with yields ranging from 67% to 95%. When the alkylating agents were methyl and ethyl sulfate or 4-nitrobenzyl chloride, even O-alkyl derivatives (**15a,b,e**) were isolated, even if the yields in this case were rather low (7% - 23%).

Finally, as confirmation of the observed behavior, the methylation of the remaining lead compounds (**2-4**) provided both products of N-alkylation and O-alkylation with yields of 26-30% (**16-18**) and 13-23% (**19-21**), respectively (**Scheme 4**).

2.2 Biology

Title compounds were evaluated in cell-based assays for cytotoxicity and antiviral activity against ssRNA+ viruses representative of the *Flaviviridae* and *Picornaviridae* families. In particular, representative viruses of two of the three genera of the *Flaviviridae* family, YFV (*Flaviviruses*) and

BVDV (*Pestiviruses*), and one genus of the *Picornaviridae* family, CVB-5 and Sb-1 (*Enteroviruses*), were tested. Compounds were also tested against other representatives of ssRNA⁺, ssRNA⁻ and DNA viruses.

Table 1 shows the overall results of the cell-based assays obtained for imidazo[4,5-*g*]quinolines (**9a-c** and **10b**), pyrido[2,3-*g*]quinoxalinones (**4**, **11a-c**, **12b**, **13c**, **14a-e**, **16-18**) and pyrido[2,3-*g*]quinoxalines (**15a,b,e**, **19-21**). Efavirenz (EFV), 2'-C-methyl-guanosine (Met-Gua), 2'-C-methyl-cytidine (Met-Cyt), 2'-C-ethynyl-cytidine (Eth-Cyt), 6-azauridine (Aza), cidofovir (CDF) and acyclovir (ACG) were used as reference compounds. As concerns the antiviral activity, none of title compounds turned out to be active against HIV-1, YFV, VSV, VV and HSV-1, although some (**9a**, **11a**, **14a**) show a modest and scattered activity against CVB-5 and Sb-1. On the contrary, compounds belonging to all classes proved to be endowed with an interesting anti-BVDV activity. Among these compounds (bold in **Table 1**), only **9c**, **11a**, **11c**, and **13c** exerted cytotoxic effects on exponentially growing MT-4 cell lines, and on MDBK and BHK cells in stationary growth, at concentrations $\leq 40 \mu\text{M}$. However, as expected, the imidazo[4,5-*g*]quinolines derivatives showed only moderate activity against BVDV. Indeed, in a previous paper our research group demonstrated the need of the presence of a chlorine atom on the quinoline ring for activity against this virus [13]. Conversely, pyrido[2,3-*g*]quinoxalines derivatives exhibited moderate to good activity towards BVDV, especially when an aryl substituent at position 3 is present in addition to the chlorine atom at position 5.

Among lead compounds, thienyl derivative **4** showed BVDV selectivity, good potency and selectivity index. For this reason, compound **4** was also tested as potential anti-HCV compound in a subgenomic replication assay. Experimental results (**Table 2**) showed that **4** was indeed able to inhibit HCV replication ($\text{EC}_{50} = 7.5 \pm 0.5 \mu\text{M}$), but was also cytotoxic for GS4.1 cells ($\text{CC}_{50} = 21 \pm 2.0 \mu\text{M}$), overall resulting in poor selectivity index (S.I. ≈ 3).

Biological analysis further confirmed that N-alkylated and O-alkylated derivatives were in general devoid of cytotoxicity. Among them, compounds **18** and **21** not only show activity greater than the corresponding unmethylated lead **4** but also are the most potent and selective molecules against BVDV with EC_{50} values of 2 and 1.3 μM , respectively.

Compound **21** was finally evaluated for its activity on the BVDV RdRp (Figure 2). *In vitro* enzymatic assay demonstrated that this compound inhibits the BVDV RNA-dependent RNA polymerase activity with an IC_{50} value of 0.64 μM , thus confirming both compound potency and viral target protein.

2.3 Modeling results

Previous enzymatic assays clearly showed that the lead compounds **1** and **2** [13] and **21** target one of the most important enzymes involved in the BVDV replication-cycle, namely the RNA-dependent RNA-polymerase (RdRp). Molecular simulation studies were then performed on a subset of 12 present compounds including the leads **1-4** with two specific purposes: i) to dissect the effect of the substitution of the quinoxalin-2(1H)-one scaffold in the corresponding N-methylated compounds **14a** and **16-18** or the 2-methoxy-quinoxaline moiety in compounds **15a** and **19-21**; and ii) the role of a bulky aromatic substituent at position 3 of the double-nitrogen ring. For this purpose, a preliminary search for a putative binding site for our compounds on the BVDV RdRp was first conducted [23-28]. In line with previous findings [26-28], the resulting portion of the enzyme making up the binding pocket for our molecular set is located between the RdRp Fingers domains 1 and 2 (residues 139–313 and 351–410, **Figure 3A**). Accordingly, all molecules were docked within the selected protein cavity according to a well-validated procedure, and the corresponding protein/drug free energies of binding (ΔG_{bind}) were scored by applying molecular dynamics (MD) simulations based on the MM/PBSA approach [23-34]. **Table 3** shows the result of the MM/PBSA analysis, from which a direct correlation between enzyme/drug affinity and *in vitro* EC₅₀ values is apparent. As seen in this Table, computational data confirm that lead compounds **1**, **2** and **4** all bind the BVDV polymerase with highly comparable affinity, while compound **3**, chosen as negative reference, does not. The critical presence of a bulky aromatic substituent at position 3 of all compounds for their optimal BVDV RdRp binding is also confirmed by the other data in Table 3. Indeed, for both series of compounds **14a,16-18** and **15a,19-21** a marked decrease in the value of ΔG_{bind} is predicted when an isopropyl group is found at that position.

To investigate in more detail the BVDV RdRp binding mode of these selected compounds, we proceeded and analyzed the main interactions involved in the stabilization of the relevant enzyme/drug complexes. Taking the quinoxaline derivative **21** as proof-of-concept, the analysis of the corresponding equilibrated MD trajectory reveals that **21** is nestled in the detected RdRp binding pocket, where it occupies two cavities lined by the side chains of residues A221, I261, I287, and Y289 and residues V216, Y303, V306, K307, P408 and A412, respectively (**Figure 3B**). Contextually, three stabilizing hydrogen bonds (HBs) are identified between donor atoms on the side chain of protein residues R295, S411 and Y674 are the corresponding counterparts in the compound structure represented by the N-pyrido atom, the nitrogen atom at position 1 of the quinoxaline moiety, and the sulfur atom of the thienyl ring, respectively (**Figure 3B**).

A quantitative analysis of the drug/protein interaction was performed via a per-residue deconvolution of the enthalpic contribution to binding afforded by each single residue involved [32-38], as reported in **Table 4**. To facilitate reading, the values of $\Delta H_{\text{bind, res}}$ for the critical RdRp residues were clustered according to a specific underlying interaction type as follows: A221, I261, I287, and Y289 belong to the first hydrophobic cavity (*HC1*), and were considered for hydrophobic (HI) and π -interactions (π). Analogously, amino acids V216, Y303, V306, K307, P408 and A412 were clustered in the other hydrophobic cavity (*HC2*) and considered for analogous interaction types. On the other hand, R295, Y674 and S411, as responsible for H-bond interactions, were classified as *HB1*, *HB2*, and *HB3*, respectively.

The permanent hydrogen bond between the N-pyrido atom of **21** and the side chain of R295 (*HB1*, average dynamic length (ADL) = 1.96 ± 0.05 Å) reflects in a stabilizing contribution of -2.03 kcal/mol. Concomitantly, the second stable H-bond interaction detected between the hydroxyl group of Y674 and the quinoxaline nitrogen atom (*HB2*, average dynamic length (ADL) = 1.94 ± 0.03 Å) provides a favorable contribution to binding of -1.98 kcal/mol. The third polar interaction *HB3*, involving the -OH on the side chain of S411 and the S atom of the thiophene ring of **21** is decidedly weaker, as confirmed by its $\Delta H_{\text{bind, res}}$ value of -0.58 and the corresponding longer ADL (2.15 ± 0.05 Å). Finally, the network of HI and π interactions, originated among the aromatic portions of **21** and the two identified receptor cavities *HC1* and *HC2*, considerably concur in stabilizing the protein/drug binding with an overall contribution of -5.95 kcal/mol.

With the aim of finding a molecular rationale for the points i) and ii) above, the same computational analysis was then applied to all remaining 11 compounds in **Table 3**. As can be seen by reconsidering all ΔG_{bind} values listed in this Table, the modification of the amide group in lead compounds **1-4** did not substantially affect their binding affinity towards the target protein. Taking the thienyl derivatives **4**, **18**, and **21** as proof-of-concept, the relevant ΔG_{bind} values are all very similar, being in the range $-8.00 \div -8.19$ kcal/mol (**Table 3**). In keeping with these results, the same compound trio exhibits an utterly comparable interactions profile against the RdRp of BVDV, as confirmed by their interaction spectra (**Figure 4A**) and their binding pose (**Figure 4B**).

It is worth noting how the interactions involving the second hydrophobic cavity (*HC2*) are not negligible, as they afford a stabilization to compound binding comparable to those originating from *HC1*. Further, taking the quinoxaline series as a meaningful example, the corresponding interaction spectra in **Figure 5A** well illustrate the importance of the presence of a bulky, aromatic substituent able to fulfill the *HC2* HI and π network. As indeed illustrated in **Figure 5A**, both the phenyl and benzyl derivatives **15a** and **19** respectively show a similar interactions spectra compared to the best

compound **21**; this, in turn, reflects in a good estimated affinity against the target RdRp (**Table 3**). Notably, the presence of a further polar interaction in the thienyl derivative **21** (*HB3*) is not a pivotal requirement for BVDV RdRp binding, but it can be eventually exploited to optimize it. On the other hand, the isopropyl group in compound **20** is too small to aptly fit the second hydrophobic cavity: this is reflected in a plummet of both its RdRp binding affinity (**Table 3**) and (even more so) in the relevant interactions with each residue involved in the binding site (**Figure 5A**). Furthermore, since the small aliphatic substituent cannot establish the required network of hydrophobic and π interactions with the side chains of the residues belonging to the *HC2*, the compound assumes an ineffective pose, which, in turn, exerts a negative influence also on the remaining portion of the BVDV RdRp binding site (**Figure 5A-B**).

2.4 Computer Aided Drug Design

Based on the computational results reported in Section 2.3, we designed 4 new potential BVDV RdRp inhibitors. Focusing on the position 3 of the molecular scaffold, we propose the replacement of the thienyl ring of lead compound **21** with other (hetero)cyclic entities theoretically able to fulfill the determined network of intermolecular interactions. For this purpose, the following moieties were selected: 2-Furanyl (**23**), 2-Naphtyl (**24**), and 2-Benzofuranyl (**25**). Compound **22**, featuring a cyclohexyl as the substituent, was also included in the design as a sort of negative control. In fact, based on the results obtained for **20**, we surmised that the presence of a flexible moiety with no heteroatoms available for hydrogen bonding with the enzyme and with a non-aromatic character should ultimately result in a drop of the corresponding enzyme/drug affinity. Applying the same computational protocol, we docked compounds **22-25** in the enzyme binding site and calculated the corresponding enzyme affinity (ΔG_{bind}). As seen from Table 5, the new derivatives **23-25** are endowed with excellent BVDV affinities (-8.43, -8.14, and -8.72 kcal/mol, respectively), whereas compound **22** shows a remarkable lower ΔG_{bind} value (-6.36 kcal/mol), as expected.

From the deconvolution of the enthalpic component of the binding free energy (ΔH_{bind} , Figure 6A), the higher affinity of the furanyl derivatives **23** compared to **21** is justified by a shorter and stronger hydrogen bond detected between the oxygen atom and the hydroxyl group of S411 ($\text{ADL} = 2.08 \pm 0.04 \text{ \AA}$), while all other interactions within the protein binding site remain unperturbed. Contextually, in the case of compound **24**, the lack of *HB3* pharmacophoric requirement is compensated by an improvement of the hydrophobic and π interaction network, ultimately resulting in the preservation of the drug affinity towards BVDV RdRp (Figure 6A). Compound **25** represents the best structural combination in that the oxygen atom of the furanyl group is engaged in a strong H-bond with S411 ($\text{ADL} = 2.06 \pm 0.03 \text{ \AA}$) whereas the aromatic portion of the moiety is nicely

encased in the *HC2*, thereby increasing the strength of the specific hydrophobic interactions (Figure 6A). Figure 6B shows a comparison of the binding mode of compounds **21** and **25** within the BVDV RdRp binding pocket.

3. Conclusions

In this work, starting from a set of lead compounds **1-4**, different series of molecules based on the 5-chloro-pyrido[2,3-*g*]quinoxalin-2(1H)-one nuclei have been synthesized, tested as antiviral agents on a series of RNA- and DNA-viruses. Overall, the results suggest that this tricyclic nuclei appear to be interesting scaffolds in the drug discovery and development processes of new antiviral agents actives against important animal and human pathogens such as BVDV and HCV.

Specifically, biological evaluation of N-methylated (**14a**, **16-18**) and O-methylated (**15a**, **19-21**) derivatives demonstrated that these compounds are endowed with good anti-BVDV activity only when they bear a phenyl or a thienyl group at position 3. Molecular modeling studies confirmed that some modifications in the structure of the synthesized quinoxalinones **1-4** are beneficial in decreasing the lead compound toxicity profiles without affecting their affinity against their target polymerase. Additionally, and maybe more important from drug development point of view, the computational approach allowed to identify important molecular determinants for the BVDV RdRp binding that could be exploited to further optimize the structure of new derivatives provided with a more potent antiviral activity. Accordingly, further developments could interest position 3 either through the introduction of different electron donor or electron withdrawing substituents on the phenyl moiety or its replacement with other heterocycles able to fulfill the determined network of intermolecular interactions. In this perspective, we designed and tested *in silico* 4 new derivatives (**22-25**) featuring different (hetero)cyclic substituents at position 3 of the general molecular scaffold. The results confirmed that compounds **23-25**, which can preserve or ameliorate the network of protein/drug intermolecular interactions, are endowed with a high affinity towards the viral enzyme. On the other hand, the free energy of binding for compound **22** plummets in the presence of a flexible, cycloaliphatic group as a result of a global detriment of the corresponding interaction network. The synthesis and the subsequent evaluation of the antiviral activity of compounds **23-25** are in progress in order to develop and characterize a new series of a more potent BVDV RdRp inhibitors. More, compound **21** is currently undergoing assays to test its druggability profile.

Acknowledgements

The authors thank the “Assessorato della Programmazione, Bilancio, Credito e Assetto del territorio, della Regione Autonoma della Sardegna (Italia)”, LEGGE REGIONALE 7 AGOSTO 2007, for financial support.

4. Experimental

4.1. Chemistry

4.1.1. General remarks

Melting points were carried out with a Köfler hot stage or Digital Electrothermal melting point apparatus and are uncorrected. Infrared spectra were recorded as nujol mulls with a Perkin-Elmer 781 IR spectrophotometer and are expressed in ν (cm^{-1}). Nuclear magnetic resonance ($^1\text{H-NMR}$) spectra were determined in CDCl_3 , $\text{DMSO-}d_6$, $\text{CDCl}_3/\text{DMSO-}d_6$ (1:3 ratio) and were recorded with a Bruker Avance III 400 NanoBay. Chemical shifts (τ scale) are reported in parts per million (ppm) downfield from tetramethylsilane (TMS) used as internal standard. Splitting patterns are designated, as follows: s, singlet; d, doublet; t, triplet; q, quadruplet; m, multiplet; br s, broad singlet; dd, double doublet. The assignment of exchangeable protons (OH and NH) was confirmed by the addition of D_2O .

^{13}C NMR were determined in $\text{DMSO-}d_6$ and were recorded at 100 MHz with Bruker Avance III 400 NanoBay. Ms spectra were performed on combined Liquid Chromatograph-Agilent 1100 series Mass Selective Detector (MSD). Analytical thin-layer chromatography (TLC) was performed on Merck silica gel F-254 plates. Pure compounds showed a single spot in TLC. For flash chromatography, Merck silica gel 60 was used with a particle size 0.040-0.063 mm (230-400 mesh ASTM). Elemental analysis were performed on a Perkin-Elmer 2400 instrument at Laboratorio di Microanalisi, Dipartimento di Chimica e Farmacia, Università degli studi di Sassari, Italy, and the results were within $\pm 0.4\%$ of theoretical values.

4.1.2. Starting material and known intermediates

The intermediates 8-Chloro-N-cyclohexylquinoline-6,7-diamine (**7b**), 8-chloroquinoline-6,7-diamine (**4a**) and 7,8-dichloro-6-nitroquinoline (**5**) were prepared according to procedure previously reported by us [13, 20, 22]. 2-Oxo-2-(thiophen-2-yl)acetic acid (**4b**), propan-1-amine (**6a**), cyclohexanamine (**6b**), cyclohexylmethanamine (**6c**), were commercially available.

4.1.3. 5-chloro-3-(thiophen-2-yl)pyrido[2,3-g]quinoxalin-2(1H)-one (**4**)

The intermediate, 6,7-diamino-8-chloroquinoline (**4a**) (2.06 mmol) of scheme 1, was dissolved in 8 mL of H₂SO₄ 10% followed by the addition of 2.06 mmol of 2-oxo-2-(thiophen-2-yl)acetic acid (**4b**). The mixture was heated at 60°C under stirring for 1h. After cooling, the orange crude precipitate was filtered off and purified by flash chromatography over silica gel eluting with a 9:1 mixture of chloroform/methanol (43% yield); m.p. >300°C (from EtOH); IR (nujol): ν 3300, 1672 cm⁻¹; ¹H NMR (CDCl₃ + DMSO-*d*₆): τ 12.90 (1H, br s, NH), 9.00 (1H, d, J = 4.4 Hz, H-7), 8.58 (1H, d, J = 4.8 Hz, H-5'), 8.43 (1H, d, J = 8.4 Hz, H-9), 7.82 (1H, d, J = 3.6 Hz, H-3'), 7.73 (1H, s, H-10), 7.62 (1H, dd, J = 8.4 and 4.4 Hz, H-8), 7.26 (1H, dd, J = 4.8 Hz and 3.6 Hz, H-4'). ¹³C-NMR (DMSO-*d*₆): δ 121.2 (CH), 122.3 (CH), 123.3 (C), 124.3 (CH), 125.3 (C), 126.4 (CH), 126.2 (CH), 127.3 (C), 132.2 (CH), 133.8 (C), 135.2 (C), 139.8 (C), 144.8 (CH), 154.2 (C), 156.3 (C). LC/MS: m/z 316 [M + 1]. Anal. Calcd. for C₁₅H₈ClN₃OS: C, 57.42; H, 2.57; N, 13.39; found C, 57.28; H, 2.49; N, 13.28.

4.1.4. General procedure for the preparation of the intermediates **7a,c**.

To a solution of 7,8-dichloro-6-nitroquinoline (**5**) (1 g, 4.1 mmol) in DMF (10 mL) an excess of the required substituted amines **6a,c** (16 mmol) was added dropwise with stirring. The solution was then stirred for further 8 h at 100°C. After cooling, water was added (10 mL) and the solution was extracted with CHCl₃. The organic extracts were dried on sodium sulfate, filtered, and the chloroform solution concentrated under reduced pressure. The oil residues were purified by flash chromatography eluting with a 8:2 mixture of petroleum ether/ethyl acetate.

4.1.4. 1. 8-Chloro-6-nitro-*N*-propylquinolin-7-amine (**7a**) This compound was obtained in 25% yield by the protocol above described; m.p. 91-93 °C (from EtOH); IR (nujol): ν 3388, 1612, 1525, 1345, cm⁻¹; ¹H NMR (CDCl₃): τ 9.05 (1H, dd, J = 4.2 and 1.6 Hz, H-2), 8.37 (1H, s, H-5), 8.14 (1H, dd, J = 8.2 and 1.6 Hz, H-4), 7.35 (1H, dd, J = 8.2 and 4.2 Hz, H-3), 5.94 (1H, br s, NH), 3.36 (2H, m, NH-CH₂-CH₂-CH₃), 1.78-1.60 (2H, m, NH-CH₂-CH₂-CH₃), 0.99 (3H, t, J = 7.4 Hz, CH₃). ¹³C-NMR (CDCl₃): δ 11.0 (CH₃), 22.2 (CH₂), 46.0 (CH₂), 114.8 (C), 121.5 (C), 122.5 (CH), 124.0 (CH), 137.6 (CH), 137.8 (C), 139.5 (C), 142.5 (C), 154.2 (CH). LC/MS: m/z 268 [M + 1]. Anal. Calcd. for C₁₂H₁₂ClN₃O₂: C, 54.25; H, 4.55; N, 15.82; found C, 54.05; H, 4.68; N, 15.69.

4.1.4. 2. 8-Chloro-N-(cyclohexylmethyl)-6-nitroquinolin-7-amine (**7c**)

This compound was obtained in 58% yield by the protocol above described; m.p. 87-89 °C (from EtOH); IR (nujol): ν 3404, 1613, 1525, 1345, cm^{-1} ; ^1H NMR (CDCl_3): τ 9.04 (1H, dd, $J = 4.2$ and 1.6 Hz, H-2), 8.34 (1H, s, H-5), 8.13 (1H, dd, $J = 8.2$ and 1.6 Hz, H-4), 7.34 (1H, dd, $J = 8.2$ and 4.2 Hz, H-3), 5.97 (1H, br s, NH), 3.20 (2H, t, CH_2), 1.76-0.9 (11H, m, cyclohexyl). ^{13}C -NMR (CDCl_3): δ 24.8 (2 x CH_2), 26.2 (CH_2), 30.8 (2 x CH_2), 37.7 (CH), 54.0 (CH_2), 113.8 (C), 120.8 (C), 121.70 (CH), 123.1 (CH), 136.9 (CH), 137.0 (C), 138.7 (C), 142.3 (C), 153.6 (CH). LC/MS: m/z 322 [M + 1]. Anal. Calcd. for $\text{C}_{16}\text{H}_{18}\text{ClN}_3\text{O}_2$: C, 60.09; H, 5.67; N, 13.14; found C, 60.32; H, 5.38; N, 13.40.

4.1.5. General procedure for the preparation of the diamines **8a,c**.

The 8-chloro-N-(substituted)-6-nitroquinolin-7-amines **7a,c** (2.07 mmol) were dissolved in 70 mL of ethanol followed by the addition of 10% Palladium on activated charcoal. This mixture was hydrogenated in Parr at 20-25°C at 3 atm. After filtering and washing the catalyst thoroughly with ethanol, the filtrates were concentrated *in vacuo* to give the desired intermediates **8a,c**.

4.1.5.1. 8-Chloro-N⁷-propylquinoline-6,7-diamine (**8a**)

This compound was obtained, as an oil, in 90% yield by the protocol described in the general procedure starting from **7a** (550 mg, 2.07 mmol); IR (nujol): ν 3450, 3330, 3240 cm^{-1} ; ^1H NMR (CDCl_3): τ 8.73 (1H, dd, $J = 4.2$ and 1.6 Hz, H-2), 7.86 (1H, dd, $J = 8.2$ and 1.6 Hz, H-4), 7.25 (1H, dd, $J = 8.2$ and 4.2 Hz, H-3), 6.87 (1H, s, H-5), 4.25 (3H, br s, NH), 3.13 (2H, t, $J = 7.2$ Hz, N- CH_2), 1.73-1.60 (2H, m, CH_2 - CH_3), 1.03 (3H, t, $J = 7.2$ Hz, CH_3). ^{13}C -NMR (CDCl_3): δ 11.0 (CH_3), 23.2 (CH_2), 46.3 (CH_2), 111.8 (C), 117.8 (CH), 118.9 (CH), 122.5 (C), 130.6 (CH), 132.9 (C), 133.6 (C), 136.2 (C), 144.0 (CH). LC/MS: m/z 238 [M + 1]. Anal. Calcd. for $\text{C}_{12}\text{H}_{14}\text{ClN}_3$: C, 61.15; H, 5.99; N, 17.83; found C, 61.01; H, 5.88; N, 17.66.

4.1.5.2. 8-chloro-N⁷-(cyclohexylmethyl)quinoline-6,7-diamine (**8c**)

This compound was obtained in 42% yield by the protocol described in the general procedure starting from **7c** (662 mg, 2.07 mmol) after flash chromatography, eluting with a 8:2 mixture of petroleum ether/ethyl acetate. M.p. 88-90 °C (from EtOH); IR (nujol): ν 3425, 3298, 3250 cm^{-1} ; ^1H NMR (CDCl_3): τ 8.74 (1H, dd, $J = 4.4$ and 1.6 Hz, H-2), 7.87 (1H, dd, $J = 8.2$ and 1.6 Hz, H-4),

7.24 (1H, dd, J = 8.0 and 4.4 Hz, H-3), 6.86 (1H, s, H-5), 4.24 (3H, br s, NH), 2.94 (2H, d, J = 7.4 Hz, CH₂) 1.95-1.04 (11H, m, cyclohexyl). ¹³C-NMR (CDCl₃): δ 24.6 (2 x CH₂), 25.8 (CH₂), 30.0 (2 x CH₂), 37.0 (CH), 54.7 (CH₂), 111.0 (C), 117.3 (CH), 118.0 (CH), 121.8 (C), 130.5 (CH), 132.8 (C), 132.0 (C), 136.2 (C), 144.2 (CH). LC/MS: m/z 292 [M + 1]. Anal. Calcd. for C₁₆H₂₀ClN₃: C, 66.31; H, 6.96; N, 14.50; found C, 66.17; H, 7.16; N, 14.22.

4.1.6. General procedure for the preparation of 2,3-substituted 3H-imidazo[4,5-g]quinolines 9a-c, 10b and the 5-chloro-2,4-substituted-pyrido[2,3-g]quinoxalin-3(4H)-ones 11a-c, 12b and 13c.

A solution of the quinolines (**8a-c**) (1.38 mmol) in ethanol (6 mL) was obtained by heating under reflux, then an excess of either required acids (2-oxo-2-phenylacetic acid, 2-oxo-2-(thiophen-2-yl)acetic acid or 2-oxo-3-phenylpropanoic acid) was added. Heating was maintained for different times as reported below. After cooling, the solution was evaporated and the crude products were purified by flash chromatography using as eluent a mixture of petroleum ether/ethyl acetate or acetone in different ratios, as reported below. The imidazo[4,5-g]quinolines **9a**, **9b**, **9c**, and **10b** were obtained associated with the pyrido[2,3-g]quinoxalines **11a**, **11b**, **13c**, and **12b**, respectively.

4.1.6.1. 2-Phenyl-3-propyl-3H-imidazo[4,5-g]quinoline (9a) and 5-chloro-2-phenyl-4-propylpyrido[2,3-g]quinoxalin-3(4H)-one (11a)

9a was obtained in 66% yield by the protocol described in the general procedure starting from **8a** (367 mg, 1.38 mmol) and 2-oxo-2-phenylacetic acid (228 mg, 1.52 mmol) for 12h. The reaction mixture was purified by silica gel column chromatography eluting with a 7:3 mixture of petroleum ether/ethyl acetate. M.p. 128-130 °C (from EtOH); TLC (petroleum ether/ethyl acetate 7:3): R_f 0.10; IR (nujol): ν 1652 cm⁻¹; ¹H NMR (CDCl₃): τ 8.91 (1H, dd, J = 3.8 and 1.6 Hz, H-6), 8.36 (1H, dd, J = 8.1 and 1.6 Hz, H-8), 8.24 (1H, s, H-4), 8.13 (1H, s, H-9), 7.82-7.77 (2H, m, H-2', 6'), 7.59-7.55 (3H, m, H-3', 4', 5'), 7.33 (1H, dd, J = 8.1 and 3.8 Hz, H-7), 4.32 (2H, t, J = 7.6 Hz, N-CH₂), 2.01-1.90 (2H, m, CH₂-CH₃), 0.91 (3H, t, J = 7.4 Hz, CH₃). ¹³C-NMR (CDCl₃): δ 11.4 (CH₃), 22.3 (CH₂), 51.7 (CH₂), 109.7 (CH), 116.9 (CH), 118.4 (CH), 124.3 (C), 128.7 (2 x CH), 129.6 (2 x CH), 130.3 (CH), 130.9 (C), 136.3(CH), 136.9 (C), 143.6 (C), 144.6 (C), 150.0 (CH), 158.4 (C). LC/MS: m/z 288 [M + 1]. Anal. Calcd. for C₁₉H₁₇N₃: C, 79.41; H, 5.96; N, 14.62; found C, 79.19; H, 5.86; N, 14.96.

11a was obtained from **8a** in 4% yield by the protocol above described. M.p. 100-102 °C (from EtOH); TLC (petroleum ether/ethyl acetate 7:3): R_f 0.24; IR (nujol): ν 1742, 1627 cm^{-1} ; ^1H NMR (CDCl_3): δ 9.06 (1H, dd, $J = 4.4$ and 2.0 Hz, H-7), 8.36 (1H, dd, $J = 8.2$ and 2.0 Hz, H-9), 8.19 (1H, s, H-10), 7.79-7.74 (2H, m, H-2', 6'), 7.60-7.57 (3H, m, H-3', 4', 5'), 7.44 (1H, dd, $J = 8.2$ Hz and $J = 4.4$ Hz, H-8), 4.66 (2H, t, $J = 7.4$ Hz, N- CH_2), 1.93-1.80 (2H, m, CH_2 - CH_3), 0.79 (3H, t, $J = 7.4$ Hz, CH_3). ^{13}C -NMR (CDCl_3): δ 11.2 (CH_3), 19.90 (CH_2), 44.1 (CH_2), 113.0 (C), 109.9 (CH), 123.0 (CH), 128.2 (C), 130.1 (2 x CH), 129.7 (2 x CH), 129.4 (C), 130.8 (CH), 134.8 (CH), 138.2 (C), 139.0 (C), 143.0 (C), 151.8 (CH), 155.4 (C), 156.0 (C). LC/MS: m/z 352 [$M + 1$]. Anal. Calcd. for $\text{C}_{20}\text{H}_{16}\text{ClN}_3\text{O}$: C, 68.67; H, 4.61; N, 12.01; found C, 68.39; H, 4.49; N, 11.79.

4.1.6.2. *3-Cyclohexyl-2-phenyl-3H-imidazo[4,5-g]quinoline (9b) and 5-chloro-4-cyclohexyl-2-phenylpyrido[2,3-g]quinoxalin-3(4H)-one (11b)*

9b was obtained in 57% yield by the protocol described in the general procedure starting from **8b** (380 mg, 1.38 mmol) and 2-oxo-2-phenylacetic acid (228 mg, 1.52 mmol) for 12h. The reaction mixture was purified by silica gel column chromatography eluting with a 7:3 mixture of petroleum ether/ethyl acetate; m.p. 183-185 °C (from EtOH); TLC (petroleum ether/ethyl acetate 7:3): R_f 0.11; IR (nujol): ν 1654 cm^{-1} ; ^1H NMR (CDCl_3): δ 8.90 (1H, dd, $J = 4.2$ and 1.6 Hz, H-6), 8.45 (1H, s, H-9), 8.36 (1H, dd, $J = 8.8$ and 1.6 Hz, H-8), 8.26 (1H, s, H-4), 7.74-7.70 (2H, m, H-2', 6'), 7.60-7.56 (3H, m, H-3', 4', 5'), 7.36 (1H, dd, $J = 8.8$ and 4.2 Hz, H-7), 4.42 (1H, m, cyclohexyl), 2.60-1.25 (10H, m, cyclohexyl). ^{13}C -NMR (CDCl_3): δ 25.1 (CH_2), 25.9 (2 x CH_2), 30.8 (2 x CH_2), 57.4 (CH), 110.2 (CH), 116.3 (CH), 118.8 (CH), 124.50 (C), 128.8 (2 x CH), 129.4 (2 x CH), 130.3 (CH), 130.4 (C), 136.7 (CH), 136.9 (C), 143.7 (C), 144.1 (C), 149.3 (CH), 158.8 (C). LC/MS: m/z 328 [$M + 1$]. Anal. Calcd. for $\text{C}_{22}\text{H}_{21}\text{N}_3$: C, 80.70; H, 6.46; N, 12.83; found C, 80.50; H, 6.30; N, 12.67.

11b was obtained from **8b** in 8% yield by the protocol above described. M.p. 169-170 °C (from EtOH); TLC (petroleum ether/ethyl acetate 7:3): R_f 0.21; IR (nujol): ν 1716, 1633 cm^{-1} ; ^1H NMR (CDCl_3): δ 9.07 (1H, dd, $J = 4.4$ and 1.6 Hz, H-7), 8.35 (1H, dd, $J = 8.2$ and 1.6 Hz, H-9), 8.17 (1H, s, H-10), 7.79-7.60 (2H, m, H-2', 6'), 7.59-7.45 (3H, m, H-3', 4', 5'), 7.42 (1H, dd, $J = 8.2$ and 4.4 Hz, H-8), 4.23 (1H, m, cyclohexyl), 2.20-1.10 (10H, m, cyclohexyl). ^{13}C -NMR (CDCl_3): δ 24.9 (CH_2), 26.4 (2 x CH_2), 33.5 (2 x CH_2), 58.7 (CH), 109.4 (CH), 123.6 (CH), 127.4 (C), 128.5 (2 x CH), 129.4 (2 x CH), 129.8 (C), 130.3 (CH), 130.8 (C), 135.7 (C), 136.8 (CH), 137.4 (C), 141.4 (C), 149.8 (CH), 153.0 (C), 160.8 (C). LC/MS: m/z 392 [$M + 1$]. Anal. Calcd. for $\text{C}_{23}\text{H}_{20}\text{ClN}_3\text{O}$: C, 70.85; H, 5.17; N, 10.78; found C, 70.62; H, 5.02; N, 10.56.

4.1.6.3. 2-Benzyl-3-(cyclohexylmethyl)-3H-imidazo[4,5-g]quinoline (**9c**) and 2-benzyl-5-chloro-4-cyclohexylpyrido[2,3-g]quinoxalin-3(4H)-one (**13c**)

9c was obtained in 9 % yield by the protocol described in the general procedure starting from **8c** (399 mg, 1.38 mmol) and 2-oxo-3-phenylpropanoic acid (249 mg, 1.52 mmol) for 6h. The reaction mixture was purified by silica gel column chromatography eluting with a 8.5:1.5 mixture of petroleum ether/acetone; m.p. 67-69 °C (from EtOH); TLC (petroleum ether/acetone 8.5:1.5): R_f 0.16; IR (nujol): ν 3451, 2360, 1632, 1600 cm^{-1} ; ^1H NMR (CDCl_3): δ 8.87 (1H, dd, $J = 4.2$ and 1.8 Hz, H-6), 8.33 (1H, dd, $J = 8.4$ and 1.8 Hz, H-8), 8.17 (1H, s, H-9), 8.00 (1H, s, H-4), 7.37-7.20 (6H, m, H-7 and H-Ph), 4.41 (2H, s, CH_2 -Ph), 3.94 (2H, d, $J = 7.6$ Hz, N- CH_2 -cyclohexyl), 2.00-0.85 (11H, m, cyclohexyl). ^{13}C -NMR (CDCl_3): δ 25.6 (2 x CH_2), 26.0 (CH_2), 31.1 (2 x CH_2), 38.0 (CH), 31.1 (CH_2), 50.6 (CH_2), 107.2 (CH), 115.8 (CH), 118.6 (CH), 127.2 (CH), 128.5 (2 x CH), 128.9 (2 x CH), 124.6 (C), 135.6 (C), 136.81 (CH), 139.1 (C), 142.7 (C), 144.5 (C), 149.2 (CH), 158.7 (C). LC/MS: m/z 356 [$M + 1$]. Anal. Calcd. for $\text{C}_{24}\text{H}_{25}\text{N}_3$: C, 81.09; H, 7.09; N, 11.82; found C, 79.90; H, 7.06; N, 11.64.

13c was obtained from **8c** in 33 % yield by the protocol above described. M.p. 53-55 °C (from EtOH); TLC (petroleum ether/acetone 8.5:1.5): R_f 0.25; IR (nujol): ν 1740, 1604 cm^{-1} ; ^1H NMR (CDCl_3): δ 9.05 (1H, dd, $J = 4.4$ and 1.6 Hz, H-7), 8.38 (1H, dd, $J = 8.2$ and 1.6 Hz, H-9), 8.19 (1H, s, H-10), 7.37-7.20 (6H, m, H-8 and H-Ph), 4.41 (2H, s, N- CH_2), 3.94 (2H, s, CH_2 -Ph), 2.00-0.85 (11H, m, cyclohexyl). ^{13}C -NMR (CDCl_3): δ 24.9 (CH_2), 26.1 (2 x CH_2), 33.80 (2 x CH_2), 52.6 (CH_2), 57.5 (CH_2), 58.8 (CH), 109.9 (CH), 123.1 (CH), 126.8 (C), 128.0 (2 x CH), 129.7 (2 x CH), 129.3 (C), 130.4 (C), 130.9 (CH), 136.1 (C), 136.3 (CH), 137.7 (C), 141.0 (C), 150.4 (CH), 153.6 (C), 155.2 (C). LC/MS: m/z 420 [$M + 1$]. Anal. Calcd. for $\text{C}_{25}\text{H}_{24}\text{ClN}_3\text{O}$: C, 71.85; H, 5.79; N, 10.05; found C, 71.59; H, 5.97; N, 10.29.

4.1.6.4. 3-Cyclohexyl-2-(thiophen-2-yl)-3H-imidazo[4,5-g]quinoline (**10b**) and 5-chloro-4-cyclohexyl-2-(thiophen-2-yl)pyrido[2,3-g]quinoxalin-3(4H)-one (**12b**)

10b was obtained in 8% yield by the protocol described in the general procedure starting from **8b** (380 mg, 1.38 mmol) and 2-oxo-2-(thiophen-2-yl)acetic acid (237 mg, 1.52 mmol) for 12h. The reaction mixture was purified by silica gel column chromatography eluting with a 6:4 mixture of petroleum ether/ethyl acetate; m.p. 152-154 °C (from EtOH); TLC (petroleum ether/ethyl acetate

7:3): R_f 0.15; IR (nujol): ν 2360, 1671 cm^{-1} ; ^1H NMR (CDCl_3): τ^m 8.89 (1H, dd, $J = 4.0$ and 1.6 Hz, H-6), 8.39 (1H, s, H-4), 8.32 (1H, dd, $J = 8.0$ and 1.6 Hz, H-8), 8.22 (1H, s, H-9), 7.63 (1H, d, $J = 5.2$ Hz, H-5'), 7.48 (1H, d, $J = 3.8$ Hz, H-3'), 7.32 (1H, dd, $J = 8.0$ and 4.0 Hz, H-7), 7.25 (1H, dd, $J = 5.2$ and 3.8 Hz, H-4'), 4.79 (1H, m, cyclohexyl), 2.72-2.50 (2H, m, cyclohexyl), 2.06-1.42 (8H, m, cyclohexyl). ^{13}C -NMR (CDCl_3): δ 25.6 (CH_2), 26.0 (2 x CH_2), 32.0 (2 x CH_2), 57.9 (CH), 105.0 (CH), 121.3 (CH), 126.70 (C), 127.1 (CH), 128.5 (CH), 128.70 (C), 128.6 (CH), 129.2 (CH), 129.10 (C), 136.0 (CH), 138.1 (C), 143.7 (C), 149.8 (CH), 158.8 (C). LC/MS: m/z 334 [$M + 1$]. Anal. Calcd. for $\text{C}_{20}\text{H}_{19}\text{N}_3\text{S}$: C, 72.04; H, 5.74; N, 12.60; found C, 71.88; H, 5.52; N, 12.85.

12b was obtained from **8b** in 30 % yield by the protocol above described. M.p. 215-217 $^\circ\text{C}$ (from EtOH); TLC (petroleum ether/ethyl acetate 7:3): R_f 0.26; IR (nujol): ν 2368, 1744, 1679 cm^{-1} ; ^1H NMR (CDCl_3): τ^m 9.07 (1H, dd, $J = 4.4$ and 1.6 Hz, H-7), 8.34 (1H, dd, $J = 8.2$ and 1.6 Hz, H-9), 8.16 (1H, s, H-10), 7.63 (1H, dd, $J = 5.0$ and 1.0 Hz, H-5'), 7.57 (1H, dd, $J = 4.0$ and 1.0 Hz, H-3'), 7.43 (1H, dd, $J = 8.2$ and 4.4 Hz, H-8), 7.24 (1H, dd, $J = 5.0$ and 4.0 Hz, H-4'), 4.28 (1H, m, cyclohexyl), 2.72-1.32 (10H, m, cyclohexyl). ^{13}C -NMR (CDCl_3): δ 24.9 (2 x CH_2), 25.6 (CH_2), 31.1 (2 x CH_2), 60.9 (CH), 113.0 (C), 109.2 (CH), 120.3 (CH), 123.8 (C), 124.1 (C), 125.3 (CH), 127.1 (CH), 127.3 (CH), 134.9 (CH), 137.6 (C), 138.3 (C), 139.4 (C), 149.3 (CH), 152.4 (C), 159.0 (C). LC/MS: m/z 398 [$M + 1$]. Anal. Calcd. for $\text{C}_{21}\text{H}_{18}\text{ClN}_3\text{OS}$: C, 63.71; H, 4.58; N, 10.61; found C, 63.98; H, 4.26; N, 10.85.

4.1.6.5. 5-chloro-4-(cyclohexylmethyl)-2-phenylpyrido[2,3-g]quinoxalin-3(4H)-one (**11c**)

This compound was obtained in 68 % yield by the protocol described in the general procedure starting from **8c** (399 mg, 1.38 mmol) and 2-oxo-2-phenylacetic acid (228 mg, 1.52 mmol) for 2h and 45'; the compound was purified by silica gel column chromatography eluting with a 6:4 mixture of petroleum ether/ethyl acetate; m.p. 129-131 $^\circ\text{C}$ (from EtOH); IR (nujol): ν 1732, 1627, 1604 cm^{-1} ; ^1H NMR (CDCl_3): τ^m 9.05 (1H, dd, $J = 4.4$ and 1.6 Hz, H-7), 8.38 (1H, dd, $J = 8.2$ and 1.6 Hz, H-9), 8.19 (1H, s, H-10), 7.80-7.72 (2H, m, H-2', 6'), 7.62-7.50 (3H, m, H-3', 4', 5'), 7.41 (1H, dd, $J = 8.2$ and 4.4 Hz, H-8), 4.59 (2H, d, $J = 7.2$ Hz, CH_2), 4.12 (1H, m, cyclohexyl), 1.95-0.85 (10H, m, cyclohexyl). ^{13}C -NMR (CDCl_3): δ 25.3 (2 x CH_2), 25.9 (CH_2), 30.9 (2 x CH_2), 45.1 (CH), 48.3 (CH_2), 115.9 (CH), 119.0 (CH), 126.1 (C), 128.2 (2 x CH), 129.9 (2 x CH), 130.4 (C), 131.1 (CH), 130.2 (C), 136.3 (C), 136.8 (CH), 138.4 (C), 142.1 (C), 148.9 (CH), 154.2 (C), 159.5 (C). LC/MS: m/z 406 [$M + 1$]. Anal. Calcd. for $\text{C}_{24}\text{H}_{22}\text{ClN}_3\text{O}$: C, 71.37; H, 5.49; N, 10.40; found C, 71.06; H, 5.68; N, 10.14.

4.1.7. General procedure for the preparation of 5-chloro-1-substituted-3-phenylpyrido[2,3-g]quinoxalin-2(1H)-ones **14a-e** and the 5-chloro-2-substituted-3-phenylpyrido[2,3-g]quinoxalines **15a,b,e**.

To a mixture of the 5-chloro-3-phenylpyrido[2,3-g]quinoxalin-2(1H)-one (**1**) [13] (492 mg, 1.60 mmol) and Cs₂CO₃(521 mg, 1.60 mmol) in anhydrous *N,N*-dimethylformamide (DMF) (10 mL) an excess of the required alkylant agents (dimethyl sulfate, diethyl sulfate, bromomethylbenzene, 1-chloromethyl-4-nitrobenzene) (1.60-7.07 mmol) in *N,N*-dimethylformamide (5-10 mL) was added dropwise. The mixture was stirred at 60°C for 1-16h, then allowed to cool to room temperature and water (50 mL) was added. The resulting precipitates were collected by filtration, washed with water and the crude products were purified by flash chromatography using a mixture of ethyl ether/methanol as eluent in different ratios as reported below. The 1-substituted-pyrido[2,3-g]quinoxalin-2(1H)-ones **14a,b,e** were obtained associated with the 2-substituted-pyrido[2,3-g]quinoxalines **15a,b,e** respectively.

4.1.7.1. 5-Chloro-1-methyl-3-phenylpyrido[2,3-g]quinoxalin-2(1H)-one (**14a**) and 5-chloro-2-methoxy-3-phenylpyrido[2,3-g]quinoxaline (**15a**)

14a was obtained in 77 % yield by the protocol described in the general procedure starting from **1** (492 mg, 1.60 mmol), Cs₂CO₃(521 mg, 1.60 mmol) and dimethyl sulfate (393 mg, 3.12 mmol) in DMF (10 mL) for 16h; the mixture was purified by silica gel column chromatography eluting with a 9.5:0.5 mixture of ethyl ether/methanol; m.p. 256-258 °C (from EtOH); TLC (petroleum ether/aceton 8.5:1.5): R_f 0.65; IR (nujol): ν 1651, 1624 cm⁻¹; ¹H NMR (CDCl₃): δ 9.00 (1H, d, J = 4.4 Hz, H-7), 8.52 (1H, d, J = 8.6 Hz, H-9), 8.17 (1H, d, J = 8.6 Hz, H-8), 7.60-7.45 (5H, m, H-Ph), 7.42 (1H, s, H-10), 3.78 (3H, s, CH₃). ¹³C-NMR (CDCl₃): δ 35.3 (CH₃), 109.1 (CH), 122.9 (CH), 128.1 (2 x CH), 128.7 (C), 129.2 (2 x CH), 130.8 (C), 131.5 (CH), 133.4 (C), 135.8 (C), 136.9 (CH), 137.9 (C), 139.2 (C), 150.0 (CH), 152.8 (C), 153.7 (C). LC/MS: m/z 324 [M + 1]. Anal. Calcd. for C₁₈H₁₂ClN₃O: C, 67.19; H, 3.76; N, 13.06; found C, 67.03; H, 3.45; N, 12.96.

15a was obtained from **1** in 19 % yield by the protocol above described. M.p. 148-150 °C (from EtOH); TLC (petroleum ether/aceton 8.5:1.5): R_f 0.46; IR (nujol): ν 1732, 1665 cm⁻¹; ¹H NMR (DMSO-*d*₆): δ 9.13 (1H, d, J = 4.2 Hz, H-7), 8.35 (1H, d, J = 8.2 Hz, H-9), 8.26 (1H, s, H-10), 8.10 (2H, m, H-2', 6'), 7.53 (4H, m, H-8, H-3', 4', 5'), 4.23 (3H, s, CH₃). ¹³C-

NMR (DMSO-*d*₆): δ 54.3 (CH₃), 120.5 (CH), 123.9 (CH), 126.1 (C), 127.0 (2 x CH), 128.3 (CH), 129.0 (2 x CH), 130.1 (CH), 130.8 (CH), 131.2 (C), 131.9 (C), 134.8 (C), 136.0 (CH), 140.1 (C), 150.1 (CH), 151.9 (C), 154.0 (C). LC/MS: *m/z* 324 [M + 1]. Anal. Calcd. for C₁₈H₁₂ClN₃O: C, 67.19; H, 3.76; N, 13.06; found C, 67.06; H, 3.54; N, 12.84.

4.1.7.2. 5-chloro-1-ethyl-3-phenylpyrido[2,3-*g*]quinoxalin-2(1*H*)-one (**14b**) and 5-chloro-2-ethoxy-3-phenylpyrido[2,3-*g*]quinoxaline (**15b**)

14b was obtained in 71 % yield by the protocol described in the general procedure starting from **1** (492 mg, 1.60 mmol), Cs₂CO₃ (521 mg, 1.60 mmol) and diethyl sulfate (284 mg, 1.84 mmol) in DMF (10 mL) for 4h; the mixture was purified by silica gel column chromatography eluting with a 9:1 mixture of ethyl ether/methanol; m.p. 252-253 °C (from EtOH); TLC (petroleum ether/acetone 8.5:1.5): *R_f* 0.70; IR (nujol): ν 1664, 1597 cm⁻¹; ¹H NMR (CDCl₃): δ 9.00 (1H, s, H-7), 8.51 (1H, d, *J* = 7.6 Hz, H-9), 8.39 (2H, m, H-2', 6'), 8.09 (1H, s, H-10), 7.60 (4H, m, H-8, H-3', 4', 5'), 4.38 (2H, q, *J* = 6 Hz, CH₂), 1.48 (3H, s, t, *J* = 7.2 Hz, CH₃). ¹³C-NMR (DMSO-*d*₆): δ 11.9 (CH₃), 37.6 (CH₂), 109.3 (CH), 123.1 (CH), 127.9 (2 x CH), 128.2 (C), 129.0 (2 x CH), 130.9 (C), 131.0 (CH), 131.2 (C), 132.6 (C), 135.5 (C), 136.2 (CH), 139.9 (C), 151.0 (CH), 153.1 (C), 154.8 (C). LC/MS: *m/z* 338 [M + 1]. Anal. Calcd. for C₁₉H₁₄ClN₃O: C, 67.96; H, 4.20; N, 12.51; found C, 68.31; H, 4.08; N, 12.88.

15b was obtained from **1** in 23 % yield by the protocol above described. M.p. 160-162 °C (from EtOH); TLC (petroleum ether/acetone 8.5:1.5): *R_f* 0.38; IR (nujol): ν 1733, 1669 cm⁻¹; ¹H NMR (DMSO-*d*₆): δ 9.04 (1H, d, *J* = 4.2 Hz, H-7), 8.51 (1H, d, *J* = 8.4 Hz, H-9), 8.27 (1H, s, H-10), 8.17 (2H, m, H-2', 6'), 7.48 (4H, m, H-8, H-3', 4', 5'), 4.55 (2H, q, *J* = 6.8 Hz, CH₂), 1.33 (3H, t, *J* = 6.8 Hz, CH₃). ¹³C-NMR (DMSO-*d*₆): δ 13.9 (CH₃), 63.3 (CH₂), 122.2 (CH), 122.7 (CH), 127.8 (C), 128.18 (2 x CH), 128.8 (C), 129.9 (2 x CH), 130.5 (CH), 131.0 (CH), 131.2 (C), 132.6 (C), 135.5 (C), 136.2 (CH), 139.9 (C), 151.0 (CH), 153.1 (C), 154.8 (C). LC/MS: *m/z* 338 [M + 1]. Anal. Calcd. for C₁₉H₁₄ClN₃O: C, 67.96; H, 4.20; N, 12.51; found C, 67.63; H, 4.08; N, 12.22.

4.1.7.3. 5-chloro-1-(4-nitrobenzyl)-3-phenylpyrido[2,3-*g*]quinoxalin-2(1*H*)-one (**14e**) and 5-chloro-2-(4-nitrobenzyloxy)-3-phenylpyrido[2,3-*g*]quinoxaline (**15e**)

14e was obtained in 67 % yield by the protocol described in the general procedure starting from **1** (492 mg, 1.60 mmol), Cs₂CO₃ (521 mg, 1.60 mmol) and 1-(chloromethyl)-4-nitrobenzene (806 mg,

4.70 mmol) in DMF (10 mL) for 4h; the mixture was purified by silica gel column chromatography eluting with a 9:1 mixture of ethyl ether/methanol; m.p. 268-270 °C (from EtOH); TLC (petroleum ether/aceton 8.5:1.5): R_f 0.61; IR (nujol): ν 1652, 1602 cm^{-1} ; ^1H NMR (CDCl_3): δ 9.09 (1H, d, $J = 4.4$ Hz, H-7), 8.51 (1H, d, $J = 7.2$ Hz, H-9), 8.61 (2H, m, H-2', H-6' Ph), 8.22 (2H, d, $J = 8.0$ Hz, H-3', H-5' benzyl), 8.10 (1H, s, H-10), 7.69 (2H, d, $J = 8.4$ Hz, H-2', H-6' benzyl), 7.60 (4H, m, H-8, H-3', H-4', H-5' Ph), 7.28, 5.75 (2H, s, CH_2). ^{13}C -NMR ($\text{DMSO-}d_6$): δ 45.5 (CH_2), 109.6 (CH), 123.2 (CH), 123.6 (2 x CH), 128.0 (2 x CH), 128.1 (2 x CH), 128.8 (C), 130.0 (2 x CH), 131.1 (C), 131.15 (CH), 131.7 (C), 132.9 (C), 135.9 (C), 136.1 (CH), 140.1 (C), 143.4 (C), 146.7 (C), 151.1 (CH), 153.8 (C), 154.9 (C). LC/MS: m/z 445 [$M + 1$]. Anal. Calcd. for $\text{C}_{24}\text{H}_{15}\text{ClN}_4\text{O}_3$: C, 65.09; H, 3.41; N, 12.65; found C, 64.91; H, 3.28; N, 12.39.

15e was obtained from **1** in 7 % yield by the protocol above described. M.p. 221-223 °C (from EtOH); TLC (petroleum ether/aceton 8.5:1.5): R_f 0.25; IR (nujol): ν 1698, 1642 cm^{-1} ; ^1H NMR ($\text{DMSO-}d_6$): δ 9.19 (1H, d, $J = 4.4$ Hz, H-7), 8.73 (2H, m, H-2', H-6' Ph), 8.45 (2H, d, $J = 8.6$ Hz, H-3', H-5' benzyl), 8.10 (1H, d, $J = 8.2$ Hz, H-9), 8.02-7.85 (5H, m, H-8, H-10, H-3', H-4', H-5' Ph), 7.36 (2H, d, $J = 8.6$ Hz, H-2', H-6' benzyl), 5.91 (2H, s, CH_2). ^{13}C -NMR ($\text{DMSO-}d_6$): δ 51.9 (CH_2), 121.8 (CH), 124.1 (CH), 124.0 (2 x CH), 126.8 (C), 127.6 (2 x CH), 128.6 (2 x CH), 128.6 (CH), 129.1 (2 x CH), 131.4 (C), 131.8 (C), 135.0 (C), 137.9 (C), 136.4 (CH), 138.6 (C), 142.6 (C), 144.1 (C), 146.6 (C), 150.3 (CH), 153.3 (C). LC/MS: m/z 445 [$M + 1$]. Anal. Calcd. for $\text{C}_{24}\text{H}_{15}\text{ClN}_4\text{O}_3$: C, 65.09; H, 3.41; N, 12.65; found C, 64.91; H, 3.23; N, 12.88.

4.1.7.4. 2-(5-chloro-2-oxo-3-phenylpyrido[2,3-g]quinoxalin-1(2H)-yl)acetonitrile (**14c**)

To a solution of the 5-chloro-3-phenylpyrido[2,3-g]quinoxalin-2(1H)-one (**1**) (492 mg, 1.60 mmol) in 2-chloroacetonitrile (12.63 mL) was added Cs_2CO_3 (658 mg, 2.02 mmol). The reaction was stirred at 60°C for 1h and then allowed to cool to room temperature. Water (50 mL) was added and the resulting precipitate was collected by filtration, washed with water and dried in a oven to give a crystalline solid. Yield: 95 %; m.p. 293-295 °C (from EtOH); IR (nujol): ν 1653, 1602 cm^{-1} ; ^1H NMR ($\text{DMSO-}d_6$): δ 9.09 (1H, d, $J = 4.4$ Hz, H-7), 8.55 (1H, d, $J = 8.6$ Hz, H-9), 8.39-8.26 (2H, m, H-2', H-6'), 8.24 (1H, s, H-10), 7.75 (1H, dd, $J = 8.6$ Hz and $J = 4.4$ Hz, H-8), 7.60-7.44 (3H, m, H-3', 4', 5'), 4.08 (2H, s, CH_2). ^{13}C -NMR ($\text{DMSO-}d_6$): δ 30.8 (CH_2), 109.2 (CH), 115.2 (C), 123.6 (CH), 128.11 (2 x CH), 128.8 (C), 129.9 (2 x CH), 130.8 (C), 131.3 (CH), 133.1 (C), 135.0 (C), 136.14 (CH), 140.4 (C), 151.4 (CH), 153.0 (C), 154.5 (C). LC/MS: m/z 349 [$M + 1$]. Anal. Calcd. for $\text{C}_{19}\text{H}_{11}\text{ClN}_4\text{O}$: C, 65.81; H, 3.20; N, 16.16; found C, 65.54; H, 3.42; N, 16.02.

4.1.7.5. 1-benzyl-5-chloro-3-phenylpyrido[2,3-g]quinoxalin-2(1H)-one (**14d**)

This compound was obtained in 30 % yield by the protocol described in the general procedure starting from **1** (492 mg, 1.60 mmol), Cs₂CO₃ (521 mg, 1.60 mmol) and (bromomethyl)benzene (1209 mg, 0.84 mL, 7.07 mmol) in DMF (10 mL) for 4h; m.p. 228-230 °C (from EtOH); IR (nujol): ν 1663, 1597 cm⁻¹; ¹H NMR (DMSO-*d*₆): τ 9.06 (1H, d, J = 4.4 Hz, H-7), 8.62 (2H, m, H-Ph), 8.12 (1H, d, J = 8.2 Hz, H-9), 7.50-7.30 (10H, m, H-8, H-10, H-Ph + benzyl), 5.56 (2H, s, CH₂). ¹³C-NMR (DMSO-*d*₆): δ 45.7 (CH₂), 109.8 (CH), 123.1 (CH), 126.9 (2 x CH), 127.3 (CH), 128.0 (2 x CH), 128.4 (2 x CH), 128.6 (CH), 129.8 (2 x CH), 131.0 (C), 131.6 (C), 132.8 (C), 135.4 (C), 136.1 (C), 139.9 (C), 151.08 (CH), 153.7 (C), 154.9 (C). LC/MS: m/z 400 [M + 1]. Anal. Calcd. for C₂₄H₁₆ClN₃O: C, 72.45; H, 4.05; N, 10.56; found C, 72.15; H, 3.87; N, 10.26.

4.1.8. General procedure for the preparation of 5-chloro-1-methyl-3-phenylpyrido[2,3-g]quinoxalin-2(1H)-ones (**16-18**) and the 5-chloro-2-methoxy-3-phenylpyrido[2,3-g]quinoxalines (**19-21**).

To a mixture of the opportune 5-chloro-3-(thiophen-2-yl)pyrido[2,3-g]quinoxalin-2(1H)-one (**4**), prepared as above reported, (502 mg, 1.60 mmol), 3-benzyl-5-chloropyrido[2,3-g]quinoxalin-2(1H)-one (**2**) [1] (515 mg, 1.60 mmol), and 5-chloro-3-isopropylpyrido[2,3-g]quinoxalin-2(1H)-one (**3**) [13] (438 mg, 1.60 mmol) and one mole equivalent of Cs₂CO₃ in anhydrous N,N-dimethylformamide (10 mL) was dropwise added an excess of dimethyl sulfate (393 mg, 3.12 mmol) in N,N-dimethylformamide (10 mL). The mixture was stirred at 60°C for 16h, then allowed to cool to room temperature and water (50 mL) was added. The resulting precipitates were collected by filtration, washed with water and the crude products were purified by flash chromatography using a mixture of ethyl ether/methanol 95:5 as eluent. The 1-methyl-pyrido[2,3-g]quinoxalin-2(1H)-ones (**16-18**) were obtained associated with the 2-methoxy-pyrido[2,3-g]quinoxalines (**19-21**) respectively.

4.1.8.1. 3-benzyl-5-chloro-1-methylpyrido[2,3-g]quinoxalin-2(1H)-one (**16**) and 3-benzyl-5-chloro-2-methoxypyrido[2,3-g]quinoxaline (**19**)

16 was obtained in 26 % yield by the protocol described in the general procedure starting from **2** [13]. M.p. 275-277 °C (from EtOH); IR (nujol): $\{$ 3315, 1652, 1607 cm^{-1} ; ^1H NMR (DMSO- d_6): $^{\text{TM}}$ 9.56 (1H, d, $J = 4.6$ Hz, H-7), 9.35 (1H, d, $J = 8.6$ Hz, H-9), 9.01 (1H, s, H-10), 8.61 (2H, m, H-2', 6'), 7.89 (1H, dd, $J = 8.6$ and 4.6 Hz, H-8), 7.71 (3H, m, H-3', 4', 5'), 3.84 (2H, s, CH_2), 3.60 (3H, s, CH_3). ^{13}C -NMR (DMSO- d_6): δ 37.5 (CH_3), 44.8 (CH_2), 109.3 (CH), 123.5 (CH), 125.3 (CH), 126.1 (C), 127.8 (C), 128.4 (2 x CH), 128.9 (2 x CH), 131.7 (C), 133.5 (CH), 134.1 (C), 136.1 (C), 140.6 (C), 145.8 (CH), 154.6 (C), 155.3 (C). LC/MS: m/z 338 [M + 1]. Anal. Calcd. for $\text{C}_{19}\text{H}_{14}\text{ClN}_3\text{O}$: C, 67.96; H, 4.20; N, 12.51; found C, 67.67; H, 4.37; N, 12.27.

19 was obtained from **2** in 23 % yield by the protocol above described. M.p. 158-160 °C (from EtOH); IR (nujol): $\{$ 3306, 1643 cm^{-1} ; ^1H NMR (DMSO- d_6): $^{\text{TM}}$ 9.71 (1H, d, $J = 4.6$ Hz, H-7), 9.38 (1H, d, $J = 8.6$ Hz, H-9), 8.95 (1H, s, H-10), 8.61 (2H, m, H-2', 6'), 7.96 (1H, dd, $J = 8.6$ and 4.6 Hz, H-8), 7.71 (3H, m, H-3', 4', 5'), 4.18 (3H, s, CH_3), 3.82 (2H, s, CH_2). ^{13}C -NMR (DMSO- d_6): δ 44.6 (CH_2), 49.8 (CH_3), 109.6 (CH), 123.7 (CH), 125.6 (CH), 126.8 (C), 128.1 (2 x CH), 128.9 (C), 130.2 (2 x CH), 132.4 (C), 135.3 (C), 136.6 (C), 135.8 (CH), 139.5 (C), 147.5 (CH), 150.6 (C), 181.5 (C). LC/MS: m/z 338 [M + 1]. Anal. Calcd. for $\text{C}_{19}\text{H}_{14}\text{ClN}_3\text{O}$: C, 67.96; H, 4.20; N, 12.51; found C, 68.25; H, 4.07; N, 12.81.

4.1.8.2. 5-chloro-3-isopropyl-1-methylpyrido[2,3-*g*]quinoxalin-2(1H)-one (**17**) and 5-chloro-3-isopropyl-2-methoxypyrido[2,3-*g*]quinoxaline (**20**)

17 was obtained, in 27 % yield by the protocol described in the general procedure starting from **3** [13]. M.p. 261-263 °C (from EtOH); IR (nujol): $\{$ 3319, 1632 cm^{-1} ; ^1H NMR (DMSO- d_6): $^{\text{TM}}$ 8.71 (1H, d, $J = 4.0$ Hz, H-7), 8.38 (1H, d, $J = 7.2$ Hz, H-9), 7.91 (1H, s, H-10), 7.74 (1H, dd, $J = 7.2$ and 4.0 Hz, H-8), 3.61 (1H, m, CH), 3.48 (3H, s, N- CH_3), 1.32 (6H, d, $J = 6.4$ Hz, 2 x CH_3). ^{13}C -NMR (CDCl_3): δ 18.2 (2 x CH_3), 37.8 (CH_3), 39.6 (CH), 109.3 (CH), 123.3 (CH), 125.1 (C), 127.7 (C), 133.2 (CH), 134.3 (C), 135.2 (C), 140.9 (C), 145.3 (CH), 154.6 (C), 155.2 (C). LC/MS: m/z 290 [M + 1]. Anal. Calcd. for $\text{C}_{15}\text{H}_{14}\text{ClN}_3\text{O}$: C, 62.61; H, 4.90; N, 14.60; found C, 62.38; H, 4.80; N, 14.34.

20 was obtained from **3** in 18 % yield by the protocol above described. M.p 153-155 °C (from EtOH); IR (nujol): $\{$ 3342, 1629 cm^{-1} ; ^1H NMR (DMSO- d_6): $^{\text{TM}}$ 8.64 (1H, d, $J = 4.0$ Hz, H-7), 8.60 (1H, d, $J = 7.2$ Hz, H-9), 8.04 (1H, s, H-10), 7.82 (1H, dd, $J = 7.2$ Hz and $J = 4.0$, H-8), 4.21 (s, 3H, OCH_3), 3.61 (1H, m, CH), 1.32 (6H, d, $J = 6.4$ Hz, 2 x CH_3). ^{13}C -NMR (DMSO- d_6): δ 19.2 (2 x CH_3), 39.7 (CH), 54.1 (CH_3), 123.0 (CH), 124.9 (C), 126.9 (CH), 128.3 (C), 132.6 (CH), 135.2 (C),

136.1 (C), 142.0 (C), 147.6 (C), 149.3 (CH), 181.8 (C). LC/MS: m/z 290 [M + 1]. Anal. Calcd. for $C_{15}H_{14}ClN_3O$: C, 62.61; H, 4.90; N, 14.60; found C, 62.57; H, 5.12; N, 14.91.

4.1.8.3. 5-chloro-1-methyl-3-(thiophen-2-yl)pyrido[2,3-g]quinoxalin-2(1H)-one (18) and 5-chloro-2-methoxy-3-(thiophen-2-yl)pyrido[2,3-g]quinoxaline (21)

18 was obtained in 30 % yield by the protocol described in the general procedure starting from **4**. M.p. 247-249 °C (from EtOH); IR (nujol): ν 3300, 1652 cm^{-1} ; 1H NMR ($CDCl_3$): δ 9.01 (1H, d, J = 4.0 Hz, H-7), 8.50 (1H, d, J = 7.0 Hz, H-5'), 8.47 (1H, d, J = 8.0 Hz, H-9), 8.04 (1H, s, H-10), 7.96 (1H, d, J = 4.2 Hz, H-3'), 7.67 (1H, dd, J = 8.0 and 4.0 Hz, H-8), 7.31 (1H, dd, J = 7.0 and 4.2 Hz, H-4'), 3.77 (3H, s, CH_3). ^{13}C -NMR ($CDCl_3$): δ 41.58 (CH_3), 109.4 (CH), 122.6 (CH), 124.0 (C), 125.1 (CH), 125.7 (C), 127.2 (CH), 127.5 (CH), 127.9 (C), 132.7 (CH), 134.4 (C), 135.7 (C), 140.2 (C), 145.6 (CH), 153.8 (C), 157.6 (C). LC/MS: m/z 330 [M + 1]. Anal. Calcd. for $C_{16}H_{10}ClN_3OS$: C, 58.63; H, 3.07; N, 12.82; found C, 58.96; H, 2.91; N, 12.68.

21 was obtained from **4** in 13 % yield by the protocol above described. M.p. 148-150 °C (from EtOH); IR (nujol): ν 3321, 1663 cm^{-1} ; 1H NMR ($CDCl_3$): δ 9.07 (1H, d, J = 4.4 Hz, H-7), 8.34 (1H, d, J = 7.0 Hz, H-5'), 8.32 (1H, d, J = 8.0 Hz, H-9), 8.07 (1H, s, H-10), 7.61 (1H, d, J = 4.2 Hz, H-3'), 7.41 (1H, dd, J = 8.0 and 4.4 Hz, H-8), 7.15 (1H, dd, J = 7.0 and 4.2 Hz, H-4'), 4.23 (3H, s, CH_3). ^{13}C -NMR ($CDCl_3$): δ 54.26 (CH_3), 109.1 (CH), 124.0 (CH), 125.8 (C), 126.3 (CH), 126.8 (C), 128.3 (CH), 128.6 (CH), 129.1 (C), 134.2 (CH), 136.6 (C), 138.2 (C), 139.8 (C), 144.9 (C), 149.4 (CH), 158.2 (C). LC/MS: m/z 330 [M + 1]. Anal. Calcd. for $C_{16}H_{10}ClN_3OS$: C, 58.63; H, 3.07; N, 12.82; found C, 59.01; H, 2.86; N, 12.94.

4.2. Biology

4.2.1 Test compounds

Compounds were dissolved in DMSO at 100 mM, and then diluted in culture medium.

4.2.2. Cells and Viruses

Cell lines were purchased from American Type Culture Collection (ATCC). The absence of mycoplasma contamination was checked periodically by the Hoechst staining method. Cell lines supporting the multiplication of RNA and DNA viruses were the following: $CD4^+$ human T-cells

containing an integrated HTLV-1 genome (MT-4); Madin Darby Bovine Kidney (MDBK) [ATCC CCL22 (NBL-1) *Bos Taurus*], Baby Hamster Kidney (BHK-21) [ATCC CCL10 (C-13) *Mesocricetus auratus*] and Monkey kidney (Vero 76) [ATCC CRL 1587 *Cercopithecus Aethiops*]. Viruses were purchased from American Type Culture Collection (ATCC), with the exception of Yellow Fever Virus (YFV) and Human Immunodeficiency Virus type-1 (HIV-1). Viruses representative of positive-sense single stranded RNAs (ssRNA⁺) were: (i) *Retroviridae*: the III_B laboratory strain of HIV-1, obtained from the supernatant of the persistently infected H9/III_B cells (NIH 1983); (ii) *Flaviviridae*: yellow fever virus (YFV) [strain 17-D vaccine (Stamaril Pasteur J07B01)] and bovine viral diarrhoea virus (BVDV) [strain NADL (ATCC VR-534)]; (iii) *Picornaviridae*: human enterovirus B [coxsackie type B5 (CV-B5), strain Faulkner, (ATCC VR-185)], and human enterovirus C [poliovirus type-1 (Sb-1), Sabin strain Chat (ATCC VR-1562)]. Viruses representative of negative-sense, single-stranded RNAs (ssRNA⁻) were: (iv) *Paramyxoviridae*: human respiratory syncytial virus (RSV) [strain A2 (ATCC VR-1540)]; (v) *Rhabdoviridae*: vesicular stomatitis virus (VSV) [lab strain Indiana (ATCC VR 158)]. The virus representative of double-stranded RNAs (dsRNA) *Reoviridae* was reovirus type-1 (Reo-1) [simian virus 12, strain 3651 (ATCC VR- 214)]. DNA virus representatives were: (vi) *Poxviridae*: vaccinia virus (VV) [strain Elstree (Lister Vaccine) (ATCC VR-1549)]; and (vii) *Herpesviridae*: human herpesvirus 1 (HSV-1) [strain KOS (ATCC VR- 1493)].

4.2.3. Cytotoxicity Assays

Cytotoxicity assays were run in parallel with antiviral assays. Exponentially growing MT-4 cells were seeded at an initial density of 1×10^5 cells/mL in 96-well plates in RPMI-1640 medium, supplemented with 10% foetal bovine serum (FBS), 100 units/mL penicillin G and 100 mg/mL streptomycin. Cell cultures were then incubated at 37 °C in a humidified, 5% CO₂ atmosphere, in the absence or presence of serial dilutions of test compounds. Cell viability was determined after 96 h at 37 °C by the 3-(4,5-dimethylthiazol-2-yl)-2,5-diphenyl-tetrazolium bromide (MTT) method [39]. MDBK and BHK cells were seeded in 96-well plates at an initial density of 6×10^5 and 1×10^6 cells/mL, respectively, in Minimum Essential Medium with Earle's salts (MEM-E), L-glutamine, 1 mM sodium pyruvate and 25 mg/L kanamycin, supplemented with 10% horse serum (MDBK) or 10% foetal bovine serum (FBS) (BHK). Cell cultures were then incubated at 37 °C in a humidified, 5% CO₂ atmosphere in the absence or presence of serial dilutions of test compounds. Cell viability was determined after 72 hrs at 37 °C by the MTT method [39]. Vero-76 cells were seeded in 96-well plates at an initial density of 4×10^5 cells/mL, in Dulbecco's Modified Eagle Medium (D-

MEM) with L-glutamine and 25 mg/L kanamycin, supplemented with 10% FBS. Cell cultures were then incubated at 37 °C in a humidified, 5% CO₂ atmosphere in the absence or presence of serial dilutions of test compounds. Cell viability was determined after 48-96 h at 37 °C by the MTT method.

4.2.4. Antiviral assays

Antiviral activity against HIV-1 was based on inhibition of virus-induced cytopathogenicity in MT-4 cells acutely infected with a multiplicity of infection (m.o.i.) of 0.01. Briefly, 50 µL of RPMI containing 1×10^4 MT-4 cells were added to each well of flat bottom microtitre trays, containing 50 µL of RPMI without or with serial dilutions of test compounds. Then, 20 µL of a HIV-1 suspension containing 100 CCID₅₀ were added. After a 4-day incubation at 37 °C, cell viability was determined by the MTT method. Antiviral activity against YFV and Reo-1 was based on inhibition of virus-induced cytopathogenicity in BHK-21 cells acutely infected with am.o.i. of 0.01. Activity of compounds activity against BVDV was based on inhibition of virus-induced cytopathogenicity in MDBK cells acutely infected with am.o.i. of 0.01. Briefly, BHK and MDBK cells were seeded in 96-well plates at a density of 5×10^4 and 3×10^4 cells/well, respectively, and were allowed to form confluent monolayers by incubating overnight in growth medium at 37 °C in a humidified CO₂ (5%) atmosphere. Cell monolayers were then infected with 50 µL of a proper virus dilution in maintenance medium [MEM-Earl with L-glutamine, 1 mM sodium pyruvate and 0.025 g/L kanamycin, supplemented with 0.5% inactivated FBS] to give an m.o.i of 0.01. After 2 hrs, 50 µL of maintenance medium, without or with serial dilutions of test compounds, were added. After a 3-4-day incubation at 37 °C, cell viability was determined by the MTT method [39].

Antiviral activity against CVB-5, Sb-1, VV, HSV-1, VSV and RSV was determined by plaque reduction assays in infected cell monolayers. To this end, Vero 76-cells were seeded in 24-well plates at a density of 2×10^5 cells/well and were allowed to form confluent monolayers by incubating overnight in growth medium [Dulbecco's Modified Eagle Medium (D-MEM) with L-glutamine and 4500 mg/L D-glucose and 0.025 g/L kanamycin, supplemented with 10% FBS] at 37 °C in a humidified CO₂ (5%) atmosphere. Then, monolayers were infected for 2 h with 250 µL of proper virus dilutions to give 50 to 100 PFU/well. Following removal of unadsorbed virus, 500 µL of maintenance medium [D-MEM with L-glutamine and 4500 mg/L Dglucose, supplemented with 1% inactivated FBS] containing 0.75% methylecellulose, without or with serial dilutions of test compounds, were added. Cultures were incubated at 37 °C for 2 (Sb-1 and VSV), 3 (CVB-5, VV

and HSV-1) or 5 days (RSV) and then fixed with PBS containing 50% ethanol and 0.8% crystal violet, washed and air-dried. Plaques were then counted.

4.2.5. Linear regression analysis

The extent of cell growth/viability and viral multiplication, at each drug concentration tested, were expressed as percentage of untreated controls. Concentrations resulting in 50% inhibition (CC_{50} or EC_{50}) were determined by linear regression analysis.

4.2.6. HCV replicon assay

A human hepatoma cell line (Huh-7) bearing the HCV genotype 1b replicon (GS4.1 cells), kindly provided by C. Seeger (Fox Chase University, Philadelphia, PA, USA) through Idenix Pharmaceuticals, was grown in D-MEM supplemented with 10% FBS, 2 mM L-glutamine, 110 mg/L sodium pyruvate, 0.1 mM non-essential amino acids, 100 U/mL penicillin, 100 μ g/mL streptomycin and 0.5 mg/mL G418 (Invitrogen). For dose-response testing, GS4.1 cells were seeded in 96-well plates at a density of 7.5×10^3 cells/well in 50 μ L medium containing twofold serial dilutions of test compounds (highest concentration, 75 μ M). Huh-7 cells lacking the HCV replicon served as negative controls. Plates were then incubated for 72 h at 37°C in a humidified, 5% CO_2 incubator. Inhibition of HCV replication was measured by quantification of the viral NS4A protein using an enzyme-linked immunosorbent assay (ELISA) as follows: plates were fixed for 1 min with 1:1 acetone-methanol, washed twice with PBS containing 0.1% Tween 20, left for 1 h at room temperature with TNE buffer containing 10% FBS, and then incubated for 2 h at 37°C with the anti-NS4A mouse monoclonal antibody A-236 (ViroGen, Watertown, MA, USA) diluted in the same buffer. After three washes with PBS containing 0.1% Tween 20, plates were incubated for 1 h at 37°C with anti-mouse immunoglobulin G-peroxidase conjugate in TNE buffer containing 10% FBS. After further washing as above, the reaction was developed with phenylenediamine (Zymed, San Francisco, CA, USA). The reaction was stopped after 30 min with 2 N H_2SO_4 and absorbance was determined at 492 nm using a Sunrise Tecan (Durham, NC, USA) spectrophotometer. EC_{50} values were determined from % inhibition vs compound concentration data, using a sigmoidal non-linear regression analysis based on four parameters, with a Tecan Magellan software. For cytotoxicity evaluation, Huh-7 and GS4.1 cells were treated with compounds as described above, and cellular viability was monitored using the Cell Titer 96 Aqueous One Solution cell proliferation

assay (Promega). CC_{50} values were determined from the % cytotoxicity versus compound concentration data with Tecan Magellan software, as described above.

4.2.7. Expression of the BVDV-NS5B Δ 24 polymerase

Expression and purification of BVDV-NS5B Δ 24 polymerase were performed as described in details in our previous work [13]. In brief, the expression plasmid encoding the His-tagged C-terminal 24-aminoacid-deleted BVDV-NS5B was introduced into the Escherichia coli strain Rosetta™ 2(DE3)pLysS (Novagene) by chemical transformation. Transformant bacteria were cultured overnight at 30 C in 5 mL of lysogeny broth (LB) supplemented with 25 μ g/mL kanamycin and 30 μ g/mL chloramphenicol. Cultures were then diluted into 1 L of LB medium additivated by the same quantities of the two antibiotics, and incubated at 30 C until the A600 reached 0.6–0.7. The culture was then induced overnight with 1 mM isopropyl- β -D-thiogalactopyranoside, after which cells were harvested by centrifugation and stored at 80 C until purification.

4.2.8. Purification of NS5B proteins

Cell pellets were thawed and immediately lysed by the addition of 10 mL of CellLytic B (Sigma). Insoluble material was removed by centrifugation at 11,000 rpm for 60 min at 4 C. The soluble extract was applied to a 5-mL column of nickel–nitrilotriacetic acid–agarose (Qiagen), previously equilibrated with the lysis buffer (50 mM NaH₂PO₄, 300 mM NaCl, 10 mM imidazole, pH 8.0). The column was washed extensively with the wash buffer (50 mM NaH₂PO₄, 300 mM NaCl, 20 mM imidazole, pH 8.0) and the protein was eluted stepwise with the elution buffer containing increasing concentration of imidazole (50 mM NaH₂PO₄, 300 mM NaCl, 50–250 mM imidazole, pH 8.0). The polypeptide composition of each column fraction was monitored via Coomassie-stained SDS–PAGE analysis. Fractions enriched in pure 6xHis-tagged NS5B protein, recovered in the 130–250 mM imidazole eluates, were pooled and dialyzed against a buffer containing 25 mM Tris–HCl, pH 7.5, 2.5 mM MgCl₂, 1 mM dithiothreitol, and 50% glycerol. Protein concentration was determined by the micro-Bradford method (Bio-Rad) using Bovine Serum Albumin (BSA) as standard. Following dialysis, the purified 6xHis-tagged BVDV-NS5B Δ 24 protein was divided into aliquots and stored at -80 C.

4.2.9 RNA-dependent RNA polymerase assay

Enzyme assays were performed in 96-well plates using 10 μ g/mL poly(rC) (GE Healthcare, formerly Amersham Biosciences) as template, 0.1 μ g/mL oligo(rG)₁₂ (Invitrogen) as primer, and 80 μ M GTP (Invitrogen) as substrate, in a 20 μ L reaction mixture containing 20 mM Tris/HCl, pH

7.0, 1 mM dithiothreitol, 25 mM NaCl, 20 U/mL RNasin (Promega), 5 mM MgCl₂, 5% DMSO, 5% glycerol, and 500 ng of the purified protein. After enzyme/drug pre-incubation for 30 min at room temperature, reactions were started by the addition of GTP. One microliter of three-fold serial dilutions of test compounds in DMSO 0.5% were added, and the samples were incubated for 120 min at 37 C (BVDV-NS5BΔ24). DMSO alone or the nucleotide analog 30-deoxyguanosine-50-triphosphate (30-dGTP) (tebu-bio) were used as negative and positive controls, respectively. Reactions were stopped by adding 2 μL of 200 mM EDTA. 138 microliters of the PicoGreen Quantitation Reagent Molecular Probes diluted 1:345 in TE (Tris/EDTA) buffer were added to each sample, followed by incubation for 5 min at room temperature in the dark. After excitation at 480 nm, fluorescence was measured at 520 nm in a fluorescence microplate reader (Infinite F200, Tecan). Effective fluorescence was calculated by subtracting the mean fluorescence of the blank samples and by converting it into % of activity. Percent of residual activity was then plotted vs compound concentrations. Dose–response curves were fit with GraphPad Prism (v. 6.00 for Windows, GraphPad Software, La Jolla California US) to obtain the drug concentration providing 50% inhibition (IC₅₀).

4.3. Computational details

All simulations were carried out using the *Pmemd* modules of Amber 14 [40], running on own CPU/GPU calculation cluster. The entire MD simulation and data analysis procedure was optimized by integrating Amber 14 in modeFRONTIER, a multidisciplinary and multiobjective optimization and design environment [41]. Molecular graphics images were produced using the UCSF Chimera package (v.1.10) [42]. The interaction spectra in **Figure 2A** and **3A** were obtained using GraphPad Prism version 6.00 for Mac OS X Yosemite, GraphPad Software, La Jolla California USA.

4.3.1. Docking procedure

The optimized structures of selected compounds **1-4**, **14a**, **15a**, **16-18** and **19-21** were docked into the BVDV RdRp binding pockets using the optimized structure of the RdRp of BVDV taken from our previous work [23-29]. All docking experiments were performed with Autodock 4.3/Autodock Tools 1.4.6 [43] on a win64 platform. The resulting docked conformations were clustered and visualized; then, in the absence of any relevant crystallographic information, the structure of each resulting complex characterized by the lowest Autodock interaction energy in the prevailing cluster was selected for further modeling.

4.3.2. Molecular Dynamics simulation

The inhibitor/RdRp complex obtained from the docking procedure was further refined in Amber 14 [40] using the quenched molecular dynamics (QMD) method as previously described [23-38]. According to QMD, the best energy configuration of each complex resulting from this step was subsequently solvated by a cubic box of TIP3P [44] water molecules extending at least 10 Å in each direction from the solute. The system was neutralized and the solution ionic strength was adjusted to the physiological value of 0.15 M by adding the required amounts of Na⁺ and Cl⁻ ions. Each solvated system was relaxed by 500 steps of steepest descent followed by 500 other conjugate-gradient minimization steps and then gradually heated to a target temperature of 300 K in intervals of 50 ps of NVT MD, using a Verlet integration time step of 1.0 fs. The Langevin thermostat was used to control temperature, with a collision frequency of 2.0 ps⁻¹. The protein was restrained with a force constant of 2.0 kcal/(mol Å), and all simulations were carried out with periodic boundary conditions. Subsequently, the density of the system was equilibrated via MD runs in the isothermal-isobaric (NPT) ensemble, with isotropic position scaling and a pressure relaxation time of 1.0 ps, for 50 ps with a time step of 1 fs. All restraints on the protein atoms were then removed, and each system was further equilibrated using NPT MD runs at 300 K, with a pressure relaxation time of 2.0 ps. Three equilibration steps were performed, each 4 ns long and with a time step of 2.0 fs. To check the system stability, the fluctuations of the root-mean-square-deviation (rmsd) of the simulated position of the backbone atoms of the BVDV RdRp protein with respect to those of the initial protein were monitored. All chemico-physical parameters and rmsd values showed very low fluctuations at the end of the equilibration process, indicating that the systems reached a true equilibrium condition. The equilibration phase was followed by a data production run consisting of 50 ns of MD simulations in the canonical (NVT) ensemble. Only the last 20 ns of each equilibrated MD trajectory were considered for statistical data collections. A total of 1000 trajectory snapshots were analyzed the each molecule/polymerase complex.

4.3.3. Free energy of binding analysis

The binding free energy, ΔG_{bind} , between the selected compounds and the BVDV RdRp was estimated by resorting to the MM/PBSA approach implemented in Amber 14. According to this well validated methodology [23-38], the free energy was calculated for each molecular species (complex, protein, and ligand), and the binding free energy was computed as the difference:

$$\Delta G_{\text{bind}} = G_{\text{complex}} - (G_{\text{protein}} + G_{\text{ligand}}) = \Delta E_{\text{MM}} + \Delta G_{\text{sol}} - T\Delta S$$

in which ΔE_{MM} represents the molecular mechanics energy, ΔG_{sol} includes the solvation free energy and $T\Delta S$ is the conformational entropy upon ligand binding. The per residue binding free energy

decomposition was performed exploiting the MD trajectory of each given compound/BVDV RdRp complex, with the aim of identifying the key residues involved in the ligand/protein interaction. This analysis was carried out using the MM/GBSA approach [45, 46], and was based on the same snapshots used in the binding free energy calculation.

References

- [1] S.J. Flint, L.W. Enquist, R.M. Krug, V.R. Racaniello, A.M. Skalka, Principles of Virology: Molecular Biology, Pathogenesis, and Control, ASM Press, Herndon, VA, 2000.
- [2] M. Woolhouse, F. Scott, Z. Hudson, R. Howey, M. Chase-Topping, Human viruses: discovery and emergence, Philosophical transactions of the Royal Society of London. Series B, Biological sciences, 367 (2012) 2864-2871.
- [3] D.M. Knipe, P.M. Howley, D.E. Griffin, Virus-Host Cell Interactions, in: W.W. Lippincott (Ed.) Fields Virology, Philadelphia, 2001, pp. 133-170.
- [4] J.M. Lane, J. Goldstein, Evaluation of 21st-century risks of smallpox vaccination and policy options, Ann. Inter. Med, 138 (2003) 488-493.
- [5] D.L. Heymann, M. Szczeniowski, K. Esteves, Re-emergence of monkeypox in Africa: a review of the past six years, Brit. Med. Bull., 54 (1998) 693-702.
- [6] Y.J. Hutin, R.J. Williams, P. Malfait, R. Pebody, V.N. Loparev, S.L. Ropp, M. Rodriguez, J.C. Knight, F.K. Tshioko, A.S. Khan, M.V. Szczeniowski, J.J. Esposito, Outbreak of human monkeypox, Democratic Republic of Congo, 1996 to 1997, Emerging infectious diseases, 7 (2001) 434-438.
- [7] T. O'Toole, Smallpox: An attack scenario, Emerging infectious diseases, 5 (1999) 540-546.
- [8] J.G. Breman, D.A. Henderson, Poxvirus dilemmas - monkeypox, smallpox, and biologic terrorism, N. Engl. J. Med., 339 (1998) 556-559.
- [9] Russia, Iraq, And Other Potential Sources of Anthrax, Smallpox, And Other Bioterrorist Weapons: Hearing Before the Committee On International Relations, in: Committee on International Relations, Washington: U.S. G.P.O., 2001.
- [10] M.R. Denison, Seeking membranes: positive-strand RNA virus replication complexes, PLoS biology, 6 (2008) e270.
- [11] P. Leyssen, E. De Clercq, J. Neyts, Perspectives for the treatment of infections with Flaviviridae, Clin. Microbiol. Rev., 13 (2000) 67-82, table of contents.
- [12] Centers for Disease Control and Prevention, Enterovirus surveillance United States 2002-2004, MMWR weekly, 55 (2006) 153-156.
- [13] A. Carta, I. Briguglio, S. Piras, P. Corona, G. Boatto, M. Nieddu, P. Giunchedi, M.E. Marongiu, G. Giliberti, F. Iuliano, S. Blois, C. Ibba, B. Busonera, P. La Colla, Quinoline tricyclic derivatives. Design, synthesis and evaluation of the antiviral activity of three new classes of RNA-dependent RNA polymerase inhibitors, Bioorgan. Med. Chem., 19 (2011) 7070-7084.
- [14] J. Paeshuyse, P. Leyssen, E. Mabery, N. Boddeker, R. Vrancken, M. Froeyen, I.H. Ansari, H. Dutartre, J. Rozenski, L.H. Gil, C. Letellier, R. Lanford, B. Canard, F. Koenen, P. Kerkhofs, R.O. Donis, P. Herdewijn, J. Watson, E. De Clercq, G. Puerstinger, J. Neyts, A novel, highly selective

inhibitor of pestivirus replication that targets the viral RNA-dependent RNA polymerase, *J. Virol.*, 80 (2006) 149-160.

[15] A.M. Di Bisceglie, J.H. Hoofnagle, Optimal therapy of hepatitis C, *Hepatology*, 36 (2002) S121-127.

[16] F. Poordad, J. McCone, Jr., B.R. Bacon, S. Bruno, M.P. Manns, M.S. Sulkowski, I.M. Jacobson, K.R. Reddy, Z.D. Goodman, N. Boparai, M.J. DiNubile, V. Sniukiene, C.A. Brass, J.K. Albrecht, J.P. Bronowicki, S.-. Investigators, Boceprevir for untreated chronic HCV genotype 1 infection, *N. Engl. J. Med.*, 364 (2011) 1195-1206.

[17] I.M. Jacobson, J.G. McHutchison, G. Dusheiko, A.M. Di Bisceglie, K.R. Reddy, N.H. Bzowej, P. Marcellin, A.J. Muir, P. Ferenci, R. Flisiak, J. George, M. Rizzetto, D. Shouval, R. Sola, R.A. Terg, E.M. Yoshida, N. Adda, L. Bengtsson, A.J. Sankoh, T.L. Kieffer, S. George, R.S. Kauffman, S. Zeuzem, A.S. Team, Telaprevir for previously untreated chronic hepatitis C virus infection, *N. Engl. J. Med.*, 364 (2011) 2405-2416.

[18] E.A. Gould, T. Solomon, Pathogenic flaviviruses, *Lancet*, 371 (2008) 500-509.

[19] C.C. Chase, G. Elmowalid, A.A. Yousif, The immune response to bovine viral diarrhea virus: a constantly changing picture, *Vet. Clin. North Am. Food Anim. Pract.*, 20 (2004) 95-114.

[20] A. Carta, M. Palomba, P. Corona, Synthesis of substituted aminoquinolines as useful intermediates for preparation of aromatic N-tricyclic systems, *Heterocycles*, 68 (2006) 1715-1722.

[21] P. Corona, S. Piras, M. Palomba, A. Carta, Synthesis of linear azolo and pyrido quinolines from quinoline derivatives, *Mini-Rev. Org. Chem.*, 5 (2008) 295-302.

[22] P. Sanna, A. Carta, G. Paglietti, Synthesis of two novel tricyclic rings: triazolo[4,5-g]quinolines and pyrido[2,3-g]quinoxalines derived from 6,7-diaminoquinolines, *Heterocycles* 53 (2000) 423-432.

[23] A. Carta, M. Loriga, G. Paglietti, M. Ferrone, M. Fermeglia, S. Pricl, T. Sanna, C. Ibba, P. La Colla, R. Loddo, Design, synthesis, and preliminary in vitro and in silico antiviral activity of [4,7]phenantrolines and 1-oxo-1,4-dihydro-[4,7]phenantrolines against single-stranded positive-sense RNA genome viruses, *Bioorgan. Med. Chem.*, 15 (2007) 1914-1927.

[24] M. Mazzei, E. Nieddu, M. Miele, A. Balbi, M. Ferrone, M. Fermeglia, M.T. Mazzei, S. Pricl, P. La Colla, F. Marongiu, C. Ibba, R. Loddo, Activity of Mannich bases of 7-hydroxycoumarin against Flaviviridae, *Bioorgan. Med. Chem.*, 16 (2008) 2591-2605.

[25] M. Tonelli, I. Vazzana, B. Tasso, V. Boido, F. Sparatore, M. Fermeglia, M.S. Paneni, P. Posocco, S. Pricl, P. La Colla, C. Ibba, B. Secci, G. Collu, R. Loddo, Antiviral and cytotoxic activities of aminoarylazo compounds and aryltriazene derivatives, *Bioorgan. Med. Chem.*, 17 (2009) 4425-4440.

[26] M. Tonelli, V. Boido, P. La Colla, R. Loddo, P. Posocco, M.S. Paneni, M. Fermeglia, S. Pricl, Pharmacophore modeling, resistant mutant isolation, docking, and MM-PBSA analysis: Combined experimental/computer-assisted approaches to identify new inhibitors of the bovine viral diarrhea virus (BVDV), *Bioorgan. Med. Chem.*, 18 (2010) 2304-2316.

[27] M. Tonelli, M. Simone, B. Tasso, F. Novelli, V. Boido, F. Sparatore, G. Paglietti, S. Pricl, G. Giliberti, S. Blois, C. Ibba, G. Sanna, R. Loddo, P. La Colla, Antiviral activity of benzimidazole derivatives. II. Antiviral activity of 2-phenylbenzimidazole derivatives, *Bioorgan. Med. Chem.*, 18 (2010) 2937-2953.

[28] G. Giliberti, C. Ibba, E. Marongiu, R. Loddo, M. Tonelli, V. Boido, E. Laurini, P. Posocco, M. Fermeglia, S. Pricl, Synergistic experimental/computational studies on arylazoamine derivatives

that target the bovine viral diarrhea virus RNA-dependent RNA polymerase, *Bioorgan. Med. Chem.*, 18 (2010) 6055-6068.

[29] A. Carta, I. Briguglio, S. Piras, G. Boatto, P. La Colla, R. Loddo, M. Tolomeo, S. Grimaudo, A. Di Cristina, R.M. Pipitone, E. Laurini, M.S. Paneni, P. Posocco, M. Fermeglia, S. Pricl, 3-Aryl-2-[1H-benzotriazol-1-yl]acrylonitriles: a novel class of potent tubulin inhibitors, *Eur. J. Med. Chem.*, 46 (2011) 4151-4167.

[30] E. Laurini, V.D. Col, M.G. Mamolo, D. Zampieri, P. Posocco, M. Fermeglia, L. Vio, S. Pricl, Homology Model and Docking-Based Virtual Screening for Ligands of the sigma1 Receptor, *ACS Med. Chem. Lett.*, 2 (2011) 834-839.

[31] M.A. Pierotti, E. Tamborini, T. Negri, S. Pricl, S. Pilotti, Targeted therapy in GIST: in silico modeling for prediction of resistance, *Nature reviews. Clin. Oncol.*, 8 (2011) 161-170.

[32] E. Laurini, D. Marson, V. Dal Col, M. Fermeglia, M.G. Mamolo, D. Zampieri, L. Vio, S. Pricl, Another brick in the wall. Validation of the sigma1 receptor 3D model by computer-assisted design, synthesis, and activity of new sigma1 ligands, *Mol. Pharm.*, 9 (2012) 3107-3126.

[33] C. Meyer, D. Schepmann, S. Yanagisawa, J. Yamaguchi, V. Dal Col, E. Laurini, K. Itami, S. Pricl, B. Wunsch, Pd-catalyzed direct C-H bond functionalization of spirocyclic sigma1 ligands: generation of a pharmacophore model and analysis of the reverse binding mode by docking into a 3D homology model of the sigma1 receptor, *J. Med. Chem.*, 55 (2012) 8047-8065.

[34] D. Zampieri, E. Laurini, L. Vio, S. Golob, M. Fermeglia, S. Pricl, M.G. Mamolo, Synthesis and receptor binding studies of some new arylcarboxamide derivatives as sigma-1 ligands, *Bioorgan. Med. Chem. Lett.*, 24 (2014) 1021-1025.

[35] F. Weber, S. Brune, K. Korpis, P.J. Bednarski, E. Laurini, V. Dal Col, S. Pricl, D. Schepmann, B. Wunsch, Synthesis, pharmacological evaluation, and sigma1 receptor interaction analysis of hydroxyethyl substituted piperazines, *J. Med. Chem.*, 57 (2014) 2884-2894.

[36] S. Brune, D. Schepmann, K.H. Klempnauer, D. Marson, V. Dal Col, E. Laurini, M. Fermeglia, B. Wunsch, S. Pricl, The sigma enigma: in vitro/in silico site-directed mutagenesis studies unveil sigma1 receptor ligand binding, *Biochemistry*, 53 (2014) 2993-3003.

[37] E. Laurini, D. Harel, D. Marson, D. Schepmann, T.J. Schmidt, S. Pricl, B. Wunsch, Identification, pharmacological evaluation and binding mode analysis of novel chromene and chromane based sigma1 receptor ligands, *Eur. J. Med. Chem.*, 83 (2014) 526-533.

[38] D. Zampieri, E. Laurini, L. Vio, M. Fermeglia, S. Pricl, B. Wunsch, D. Schepmann, M.G. Mamolo, Improving selectivity preserving affinity: new piperidine-4-carboxamide derivatives as effective sigma-1-ligands, *Eur. J. Med. Chem.*, 90 (2015) 797-808.

[39] R. Pauwels, J. Balzarini, M. Baba, R. Snoeck, D. Schols, P. Herdewijn, J. Desmyter, E. De Clercq, Rapid and automated tetrazolium-based colorimetric assay for the detection of anti-HIV compounds, *J. Virol. Methods*, 20 (1988) 309-321.

[40] D.A. Case, V. Babin, J.T. Berryman, R.M. Betz, Q. Cai, D.S. Cerutti, I. Cheatham, T.E., T.A. Darden, R.E. Duke, H. Gohlke, A.W. Goetz, S. Gusarov, N. Homeyer, P. Janowski, J. Kaus, I. Kolossváry, A. Kovalenko, T.S. Lee, S. LeGrand, T. Luchko, R. Luo, B. Madej, K.M. Merz, F. Paesani, D.R. Roe, A. Roitberg, C. Sagui, R. Salomon-Ferrer, G. Seabra, C.L. Simmerling, W. Smith, J. Swails, R.C. Walker, J. Wang, R.M. Wolf, X. Wu, K. P.A., AMBER 14, in, University of California, San Francisco, USA., 2014.

[41] http://www.esteco.com/home/mode_frontier/mode_frontier.html, in.

- [42] E.F. Pettersen, T.D. Goddard, C.C. Huang, G.S. Couch, D.M. Greenblatt, E.C. Meng, T.E. Ferrin, UCSF Chimera--a visualization system for exploratory research and analysis, *J. Comput. Chem.*, 25 (2004) 1605-1612.
- [43] G.M. Morris, R. Huey, W. Lindstrom, M.F. Sanner, R.K. Belew, D.S. Goodsell, A.J. Olson, AutoDock4 and AutoDockTools4: Automated docking with selective receptor flexibility, *J. Comput. Chem.*, 30 (2009) 2785-2791.
- [44] W.L. Jorgensen, J. Chandrasekhar, J.D. Madura, R.W. Impey, M.L. Klein, Comparison of simple potential functions for simulating liquid water, *J. Chem. Phys.*, 79 (1983) 926-935.
- [45] V. Tsui, D.A. Case, Theory and applications of the generalized Born solvation model in macromolecular simulations, *Biopolymers*, 56 (2000) 275-291.
- [46] A. Onufriev, D. Bashford, D.A. Case, Modification of the generalized born model suitable for macromolecules, *J. Phys. Chem. B*, 104 (2000) 3712-3720.

CAPTIONS

Fig. 1. Chemical structure of lead compounds **1-4**.

Fig. 2. Dose–response curve for compound **21** obtained from *in vitro* enzyme assay with the BVDV RNA-dependent RNA polymerase.

Fig. 3. (A) Overall representation of the BVDV RdRp molecular surface with compound **21** docked into the protein putative binding site. The inhibitor is in orange sphere representation while the protein is represented by its different domains highlighted by different colors as follows: N-terminal (residues 92-138, red), Finger domain 1 (139-313, dim gray), Palm domain 1 (314-350, green), Finger domain 2 (351-410, dark slate gray), Palm domain 2 (411-500, spring green), and Thumb domain (501-679, dark slate blue). (B) Details of compound **21** in the RdRp binding pocket. Compound **21** is depicted as atom-colored sticks-and-balls (C, gray, N, blue, Cl, green, S, yellow) Hydrogen bonds are highlighted as black broken lines. The side chains of all residues that form the primary binding pocket interacting with **21** are highlighted as colored sticks: A221, I261, I287 and Y289, medium purple; R296, spring green; V216, Y303, V306, K307, P408 and A412, magenta; S411, chartreuse; Y674, green. In both panels, hydrogen atoms, water molecules, ions and counterions are omitted for clarity.

Fig. 4. (A) Comparison of the per residue binding enthalpy decomposition $\Delta H_{\text{bind, res}}$ for compounds **4**, **18**, and **21** in complex with the BVDV RdRp. Critical receptor residues are clustered according to the specific underlying interactions: *HC* (hydrophobic cavity) and *HB* (hydrogen bond) (see legend and main text for more details). (B) Superposition of equilibrated MD snapshots of the BVDV RdRp in complex with **21** (firebrick) and **4** (cyan). Hydrogen atoms, water molecules, ions and counterions are omitted for clarity.

Fig. 5. (A) Comparison of per residue binding enthalpy decomposition for compounds **15a**, **19**, **20**, and **21** in complex with the BVDV RdRp. Critical receptor residues are clustered according to the specific underlying interactions: *HC* (hydrophobic cavity) and *HB* (hydrogen bond). (see the legend and main text for more details). (B) Superposition of equilibrated MD snapshots of the BVDV RdRp in complex with **21** (firebrick) and **20** (olive drab). Hydrogen atoms, water molecules, ions and counterions are omitted for clarity.

Fig. 6. (A) Comparison of the per residue binding enthalpy decomposition $\Delta H_{\text{bind, res}}$ for compounds **21-25** in complex with the BVDV RdRp. Critical receptor residues are clustered according to the specific underlying interactions: *HC* (hydrophobic cavity) and *HB* (hydrogen bond) (see legend and main text for more details). (B) Superposition of equilibrated MD snapshots of the BVDV RdRp in complex with **21** (firebrick) and **25** (dark slate blue). Hydrogen atoms, water molecules, ions and counterions are omitted for clarity.

Scheme 1. Synthesis of lead compound **4**. (i) H₂SO₄ 10%, 60°C, 1h.

Scheme 2. Synthesis of compounds **9a-c**, **10b**, **11a-c**, **12b**, and **13c**. Reagents and conditions: (i) DMF, 100°C, 8h. (ii) 10% Pd/C, H₂, EtOH. (iii) EtOH, reflux for 2 h to 12 h.

Scheme 3. Synthesis of compounds **14a-e** and **15a,b,e**. Reagents and conditions: (a) (CH₃)₂SO₄, DMF, Cs₂CO₃, 60°C for 16h. (b) (C₂H₅)₂SO₄, DMF, Cs₂CO₃, 60°C for 4h. (c) ClCH₂CN, 60°C, Cs₂CO₃, for 1h. (d) BrCH₂Ph, DMF, Cs₂CO₃, 60°C for 4h. (e) ClCH₂-4-(NO₂)Ph, DMF, Cs₂CO₃, 60°C for 4h.

Scheme 4. Synthesis of compounds **16-21**.

Table 1. Cytotoxicity and antiviral activity of pyrido[2,3-*g*]quinoxalines (**1-4**, **11a-c**, **12b**, **13c**, **14a-e**, **15a,b,e**, **16-21**) and imidazo[4,5-*g*]quinolines (**9a-c** and **10b**) against ssRNA⁺ (HIV-1, BVDV, YFV, CV-5, Sb-1), ssRNA⁻ (RSV, VSV), dsRNA (Reo-1) and DNA (VV, HSV-1) viruses.

Table 2. Comparative activity of compounds **1**, **2**, and **4** against BVDV and HCV in cell-based assays.

Table 3. Free energy components (ΔH_{bind} and $-T\Delta S$) and total binding free energies (ΔG_{bind}) for the 12 selected compounds in complex with the BVDV RdRp. The last row shows the correlation between the predicted ΔG_{bind} values (kcal/mol) and the corresponding experimental EC₅₀ (μM) ($R^2 = 0.89$).

Table 4. Clustered per-residue enthalpy contribution to binding ($\Delta H_{\text{bind,res}}$) for compound **21** in complex with the BVDV RdRp. All values are in kcal/mol. Errors are in the range 0.01–0.04.

Table 5. Free energy components (ΔH_{bind} and $-T\Delta S$) and total binding free energies (ΔG_{bind}) for **21** and the 4 new designed compounds in complex with the BVDV RdRp.

17	>100	>100	>100	>100	>100	>100	>100	>100	>100	>100	>100	>100	>100	>100	>100
18	>100	>100	>100	2	>100	>100	>100	>100	>100	>100	>100	>100	>100	>100	>100
19	>100	>100	>100	6	>100	>100	>100	>100	>100	>100	>100	>100	>100	>100	>100
20	>100	>100	>100	>100	>100	>100	>100	>100	>100	>100	>100	>100	>100	>100	>100
21	>100	>100	>100	1.3	>100	>100	>100	>100	>100	>100	>100	>100	>100	>100	>100
EFV	40	0.002													
Met-Gua			>100		1.1	>100		1.9							
Met-Cyt								>100	16						
Eth-Cyt										>100	27	23			
Aza										≥12.5			1.2		
CDF										>100					19
ACG										>100					3

Data represent mean values for three independent determinations. Variation among duplicate samples was less than 15%.

In bold the compounds with higher activity.

ND = Not determined.

^a Compound concentration (μM) required to reduce the proliferation of mock-infected MT-4 cells by 50%, as determined by the MTT method.

^b Compound concentration (μM) required to achieve 50% protection of MT-4 cells from HIV-1 induced cytopathogenicity, as determined by the MTT method.

^c Compound concentration (μM) required to reduce the viability of mock-infected MDBK (Bovine normal kidney) cells by 50%, as determined by the MTT method.

^d Compound concentration (μM) required to achieve 50% protection of MDBK cells from BVDV-induced cytopathogenicity, as determined by the MTT method.

^e Compound concentration (μM) required to reduce the viability of mock-infected BHK (Hamster normal kidney fibroblast) monolayers by 50%, as determined by the MTT method.

^f Compound concentration (μM) required to achieve 50% protection of BHK cells from YFV-induced cytopathogenicity, as determined by the MTT method.

^g Compound concentration (μM) required to achieve 50% protection of BHK cells from Reo-1-induced cytopathogenicity, as determined by the MTT method.

^h Compound concentration (μM) required to reduce the viability of mock-infected VERO-76 cells by 50% as determined by the MTT method.

ⁱ Compound concentration (μM) required to reduce the plaque number of CVB-5 by 50% in VERO-76 monolayers.

^l Compound concentration (μM) required to reduce the plaque number of Sb-1 by 50% in VERO-76 monolayers.

^m Compound concentration (μM) required to reduce the plaque number of RSV by 50% in VERO-76 monolayers.

ⁿ Compound concentration (μM) required to reduce the plaque number of VSV by 50% in VERO-76 monolayers.

^o Compound concentration (μM) required to reduce the plaque number of VV by 50% in VERO-76 monolayers.

^p Compound concentration (μM) required to reduce the plaque number of HSV-1 by 50% in VERO-76 monolayers.

EFV = *Efavirenz*

MetGua = 2'-C-methyl-guanosine

Met-Cyt = 2'-C-methyl-cytidine

Eth-Cyt= 2'-C-ethynyl-cytidine

Aza = 6-aza-uridine

CDF = Cidofovir

ACG = Acycloguanosine

ACCEPTED MANUSCRIPT

Table 2: Comparative activity of compounds **1**, **2**, and **4** against BVDV and HCV in cell-based assays.

Cps	Cell-based ^a					
	BVDV			HCV-1b		
	(μM)		S.I.	(μM)		S.I.
CC ₅₀ ^b	EC ₅₀ ^c	CC ₅₀ ^d		EC ₅₀ ^e		
1	>100	5 ± 0.1	>20	11 ± 1.3	>11	1
2	>100	2.6 ± 0.3	>34	65 ± 9.0	>65	1
4	>100	6 ± 0.2	>16	21 ± 2.0	7.5±0.6	3

Data represent mean values for three independent determinations.

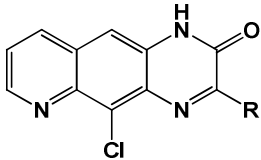
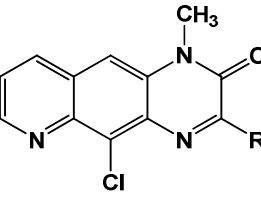
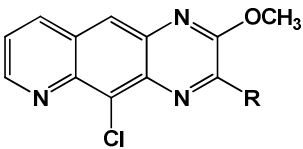
^b Compound concentration (IM) required to reduce the viability of mock-infected MDBK cells by 50%, as determined by the MTT method.

^c Compound concentration (IM) required to achieve 50% protection of MDBK cells from BVDV-induced cytopathogenicity, as determined by the MTT method.

^d Compound concentration (IM) required to reduce the viability of GS4.1 cells by 50%, as described in the Section 4.2..

^e Compound concentration (IM) required to achieve 50% protection of GS4.1 cells from cytopathogenicity, as described in the Section 4.2.

Table 3. Free energy components (ΔH_{bind} and $-T\Delta S$) and total binding free energies (ΔG_{bind}) for the 12 selected compounds in complex with the BVDV RdRp. The last row shows the correlation between the predicted ΔG_{bind} values (kcal/mol) and the corresponding experimental EC_{50} (μM) ($R^2 = 0.89$).

Scaffold	Compound	R	ΔH_{bind} (kcal/mol)	$-T\Delta S$ (kcal/mol)	ΔG_{bind} (kcal/mol)
	1	Ph	-21.50 (0.18)	13.47 (0.26)	-8.03 (0.32)
	2	Bz	-21.58 (0.19)	13.42 (0.28)	-8.16 (0.34)
	3	CH(CH ₃) ₂	-18.33 (0.16)	12.98 (0.26)	-5.35 (0.31)
	4	2-Thienyl	-21.39 (0.15)	13.39 (0.25)	-8.00 (0.29)
	14a	Ph	-20.97 (0.19)	13.51 (0.27)	-7.46 (0.33)
	16	Bz	-21.10 (0.19)	13.54 (0.29)	-7.56 (0.35)
	17	CH(CH ₃) ₂	-18.34 (0.17)	13.09 (0.25)	-5.25 (0.30)
	18	2-Thienyl	-21.36 (0.18)	13.28 (0.26)	-8.08 (0.32)
	15a	Ph	-21.37 (0.20)	13.45 (0.24)	-7.92 (0.31)
	19	Bz	-21.42 (0.18)	13.59 (0.28)	-7.83 (0.33)
	20	CH(CH ₃) ₂	-18.28 (0.16)	12.88 (0.29)	-5.40 (0.33)
	21	2-Thienyl	-21.56 (0.17)	13.37 (0.25)	-8.19 (0.30)

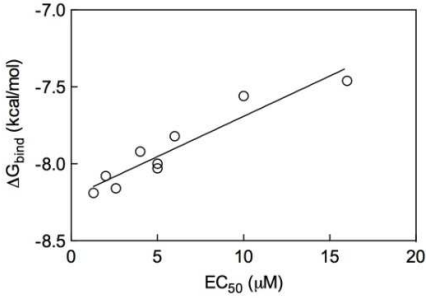
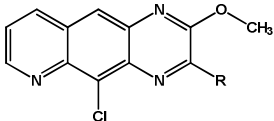
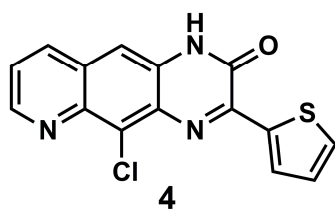
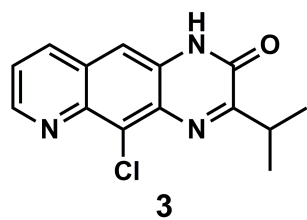
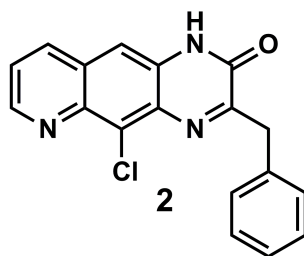
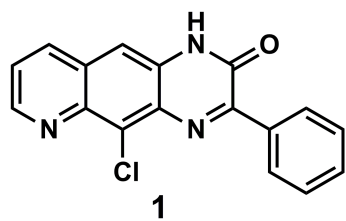


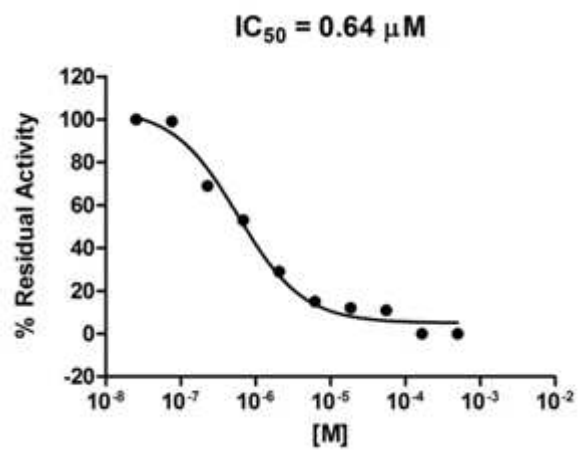
Table 4. Clustered per-residue enthalpy contribution to binding ($\Delta H_{\text{bind, res}}$) for compound **21** in complex with the BVDV RdRp. All values are in kcal/mol. Errors are in the range 0.01–0.04.

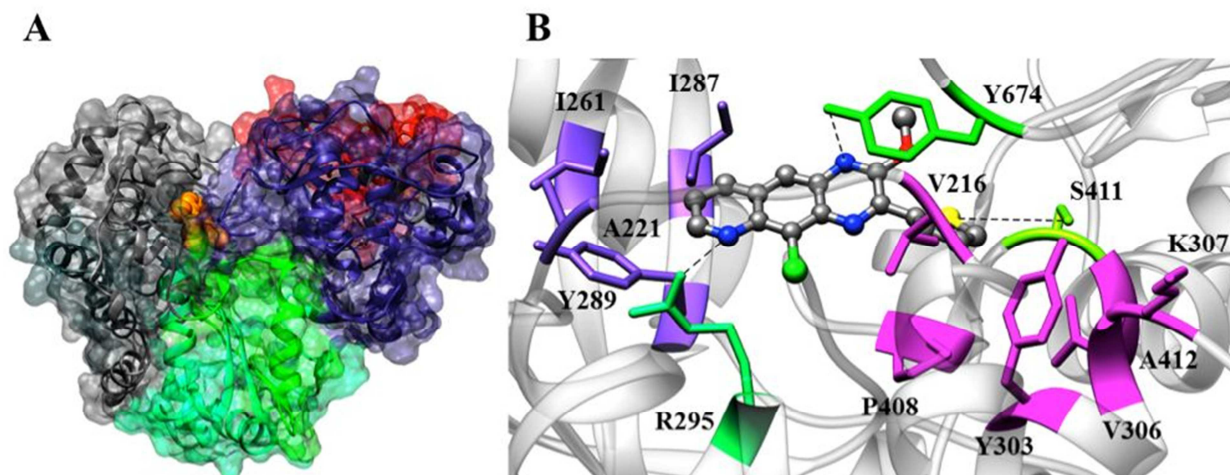
Clustered energy	<i>HC1</i>	<i>HB1</i>	<i>HB2</i>	<i>HC2</i>	<i>HB3</i>
$\Delta H_{\text{bind, res}}$	-2.98	-2.03	-1.98	-2.97	-0.58

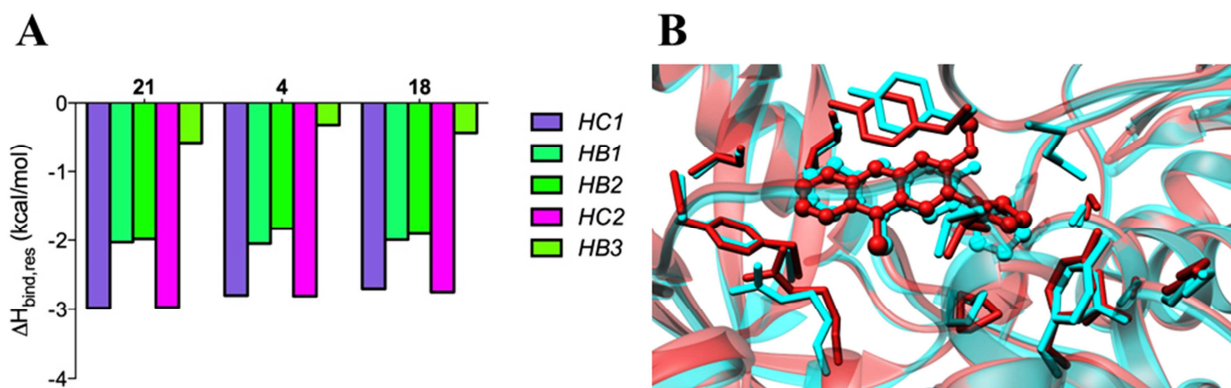
Table 5. Free energy components (ΔH_{bind} and $-T\Delta S$) and total binding free energies (ΔG_{bind}) for **21** and the 4 new designed compounds in complex with the BVDV RdRp.

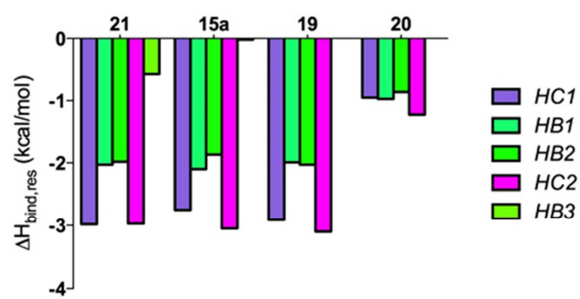
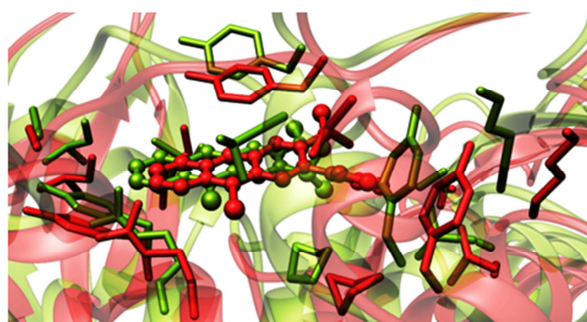
Scaffold	Compound	R	ΔH_{bind} (kcal/mol)	$-T\Delta S$ (kcal/mol)	ΔG_{bind} (kcal/mol)
	21	2-Thienyl	-21.56 (0.17)	13.37 (0.25)	-8.19 (0.30)
	22	Cyclohexyl	-20.01 (0.16)	13.65 (0.29)	-6.36 (0.33)
	23	2-Furanyl	-21.85 (0.15)	13.42 (0.27)	-8.43 (0.31)
	24	2-Naphtyl	-21.63 (0.18)	13.49 (0.26)	-8.14 (0.32)
	25	2-Benzofuranyl	-22.12 (0.15)	13.40 (0.25)	-8.72 (0.29)

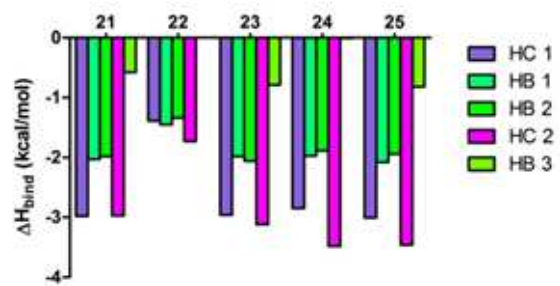
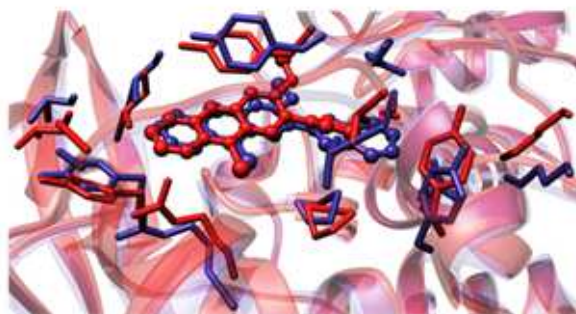




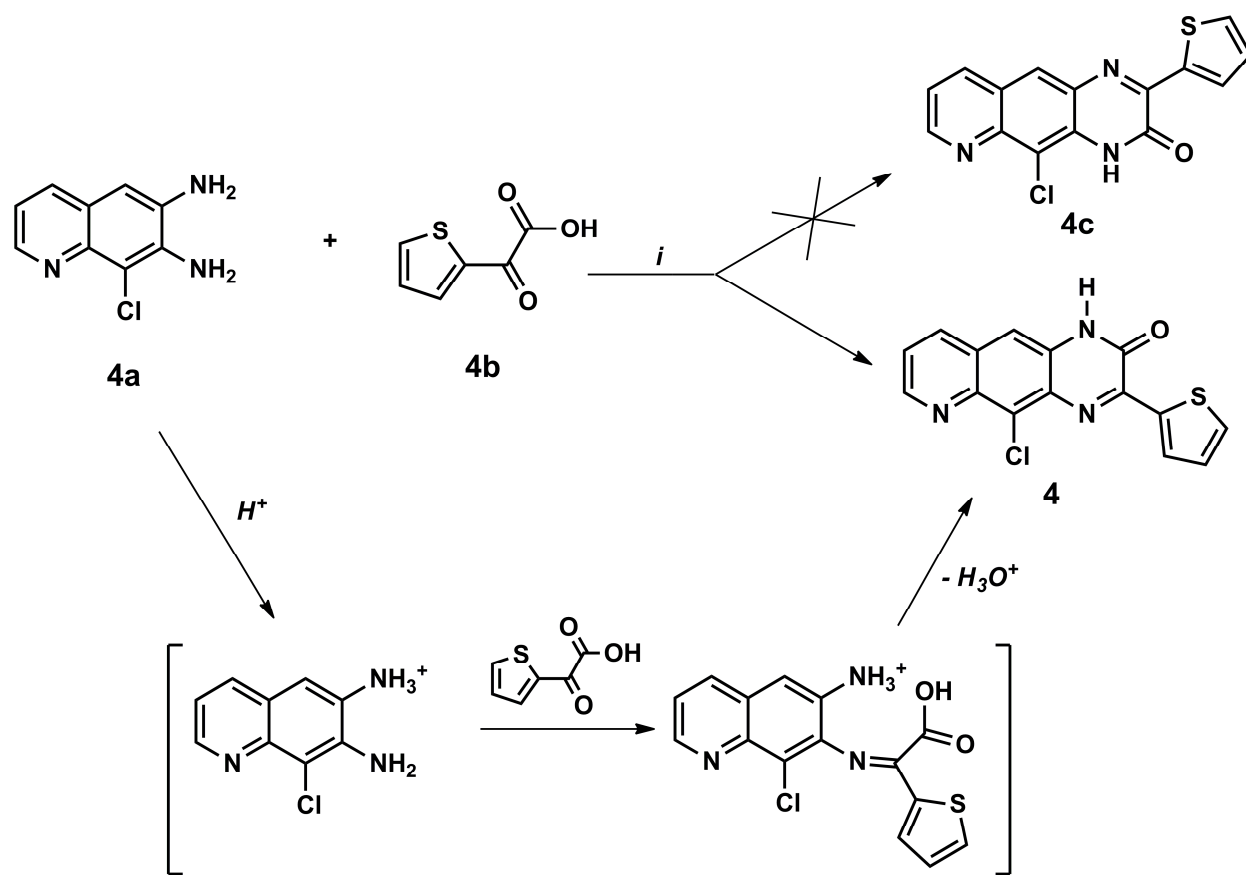


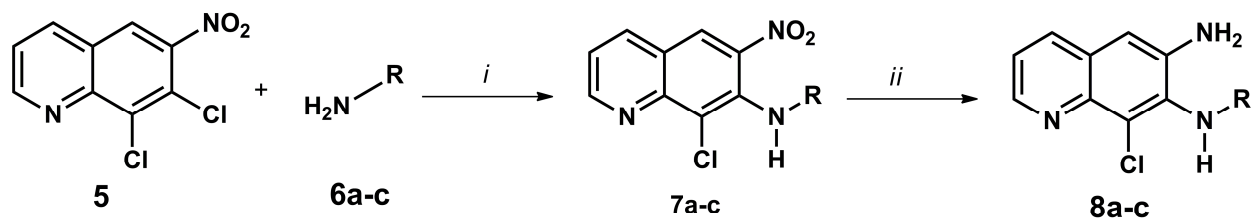


A**B**

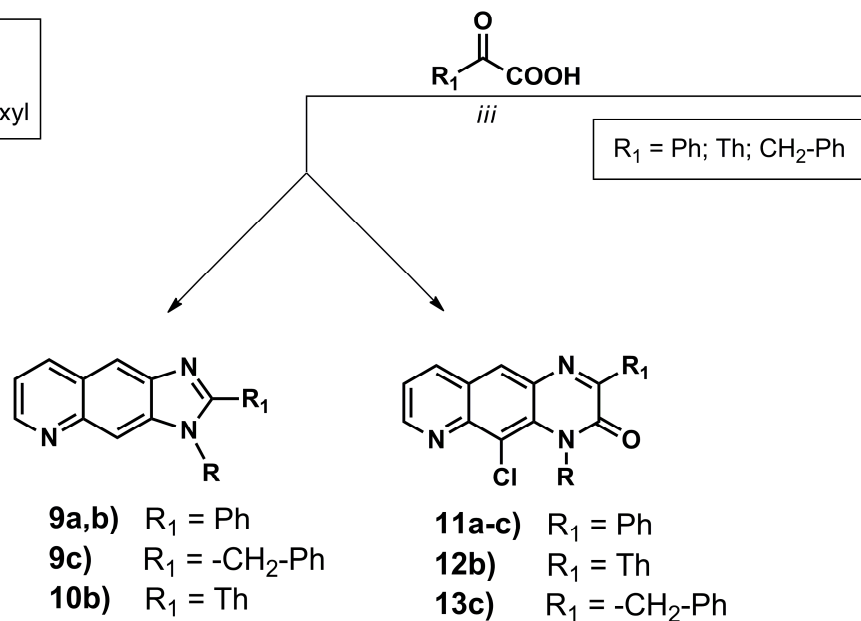
A**B**

ACCEPTED MANUSCRIPT

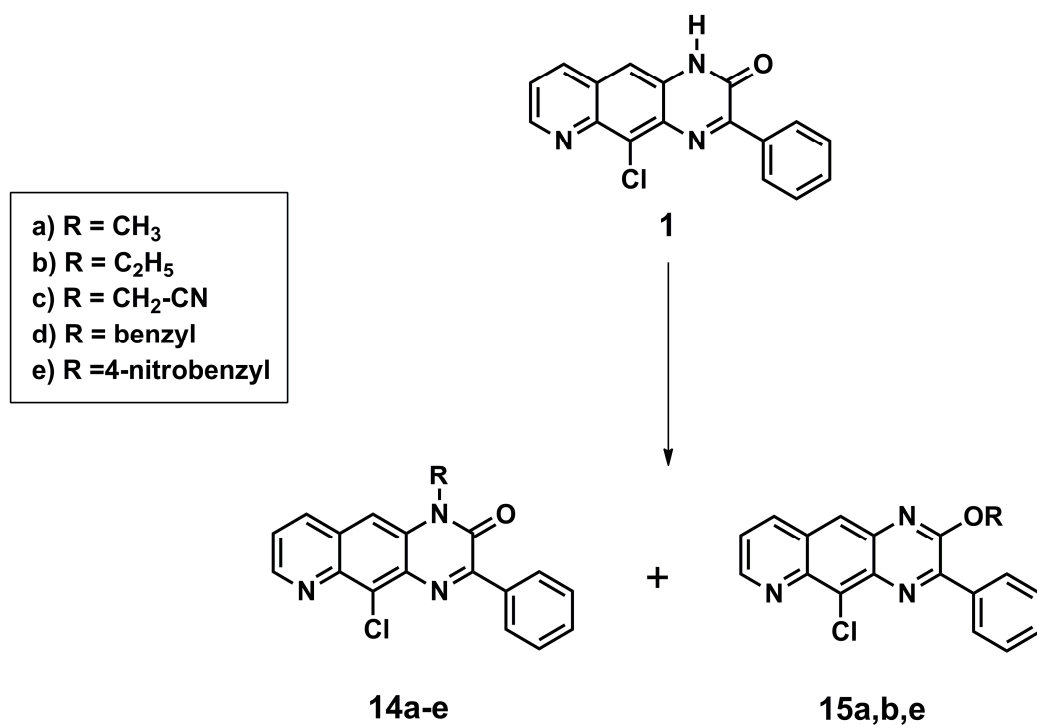


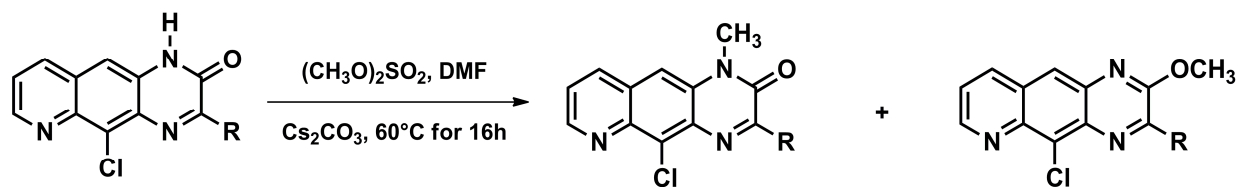


- a) R = C₃H₇
 b) R = cyclohexyl
 c) R = -CH₂-cyclohexyl



ACCEPTED





2) R = $-\text{CH}_2\text{-Ph}$

3) R = $-\text{CH}(\text{CH}_3)_2$

4) R = Th

16) R = $-\text{CH}_2\text{-Ph}$

17) R = $-\text{CH}(\text{CH}_3)_2$

18) R = Th

19) R = $-\text{CH}_2\text{-Ph}$

20) R = $-\text{CH}(\text{CH}_3)_2$

21) R = Th

Highlights

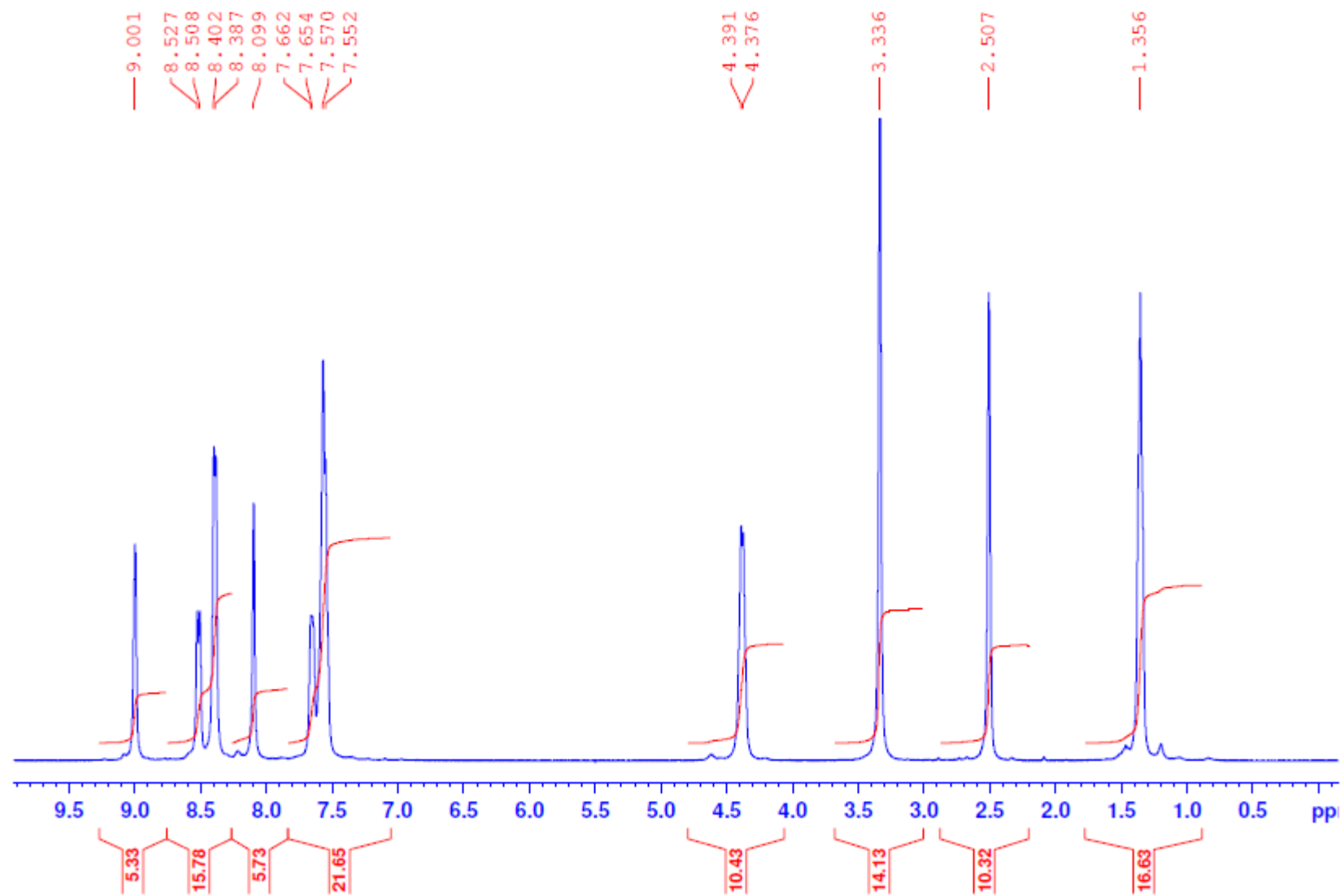
In this study we prepared imidazo[4,5-g]quinoline and pyrido[2,3-g]quinoxaline derivatives.

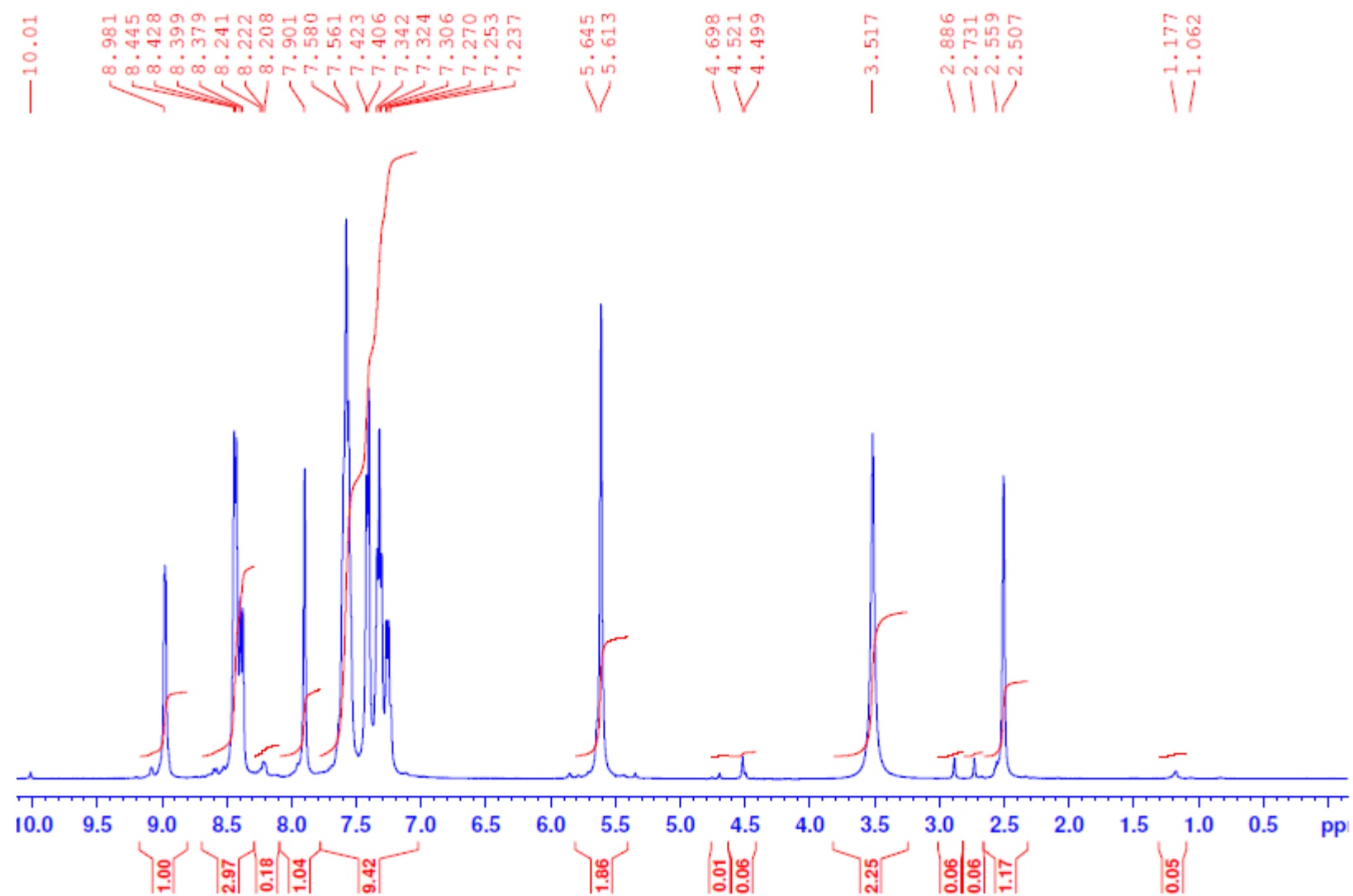
All derivatives have been investigated for their antiviral activity.

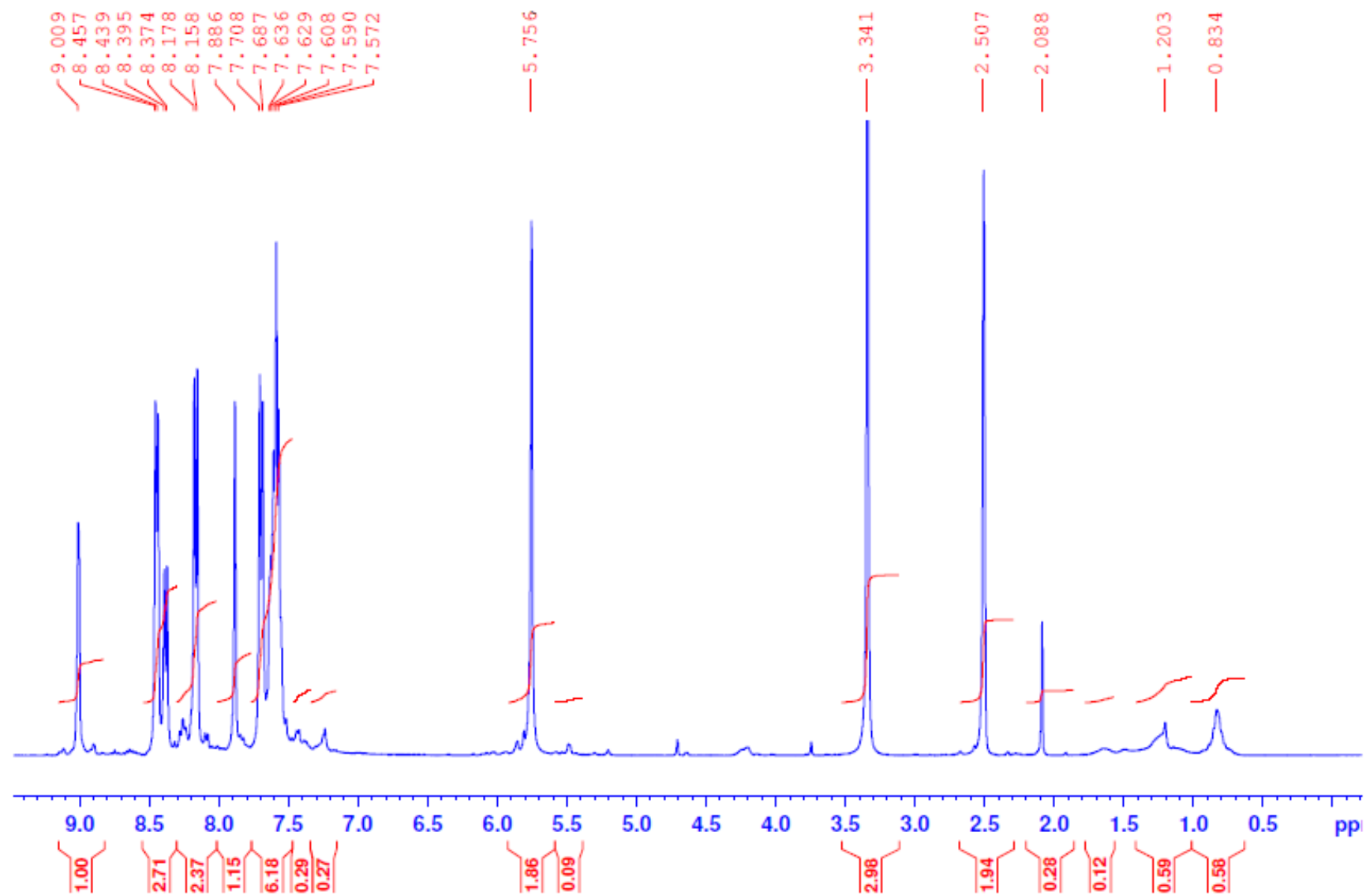
Several compounds showed micromolar activity against BVDV.

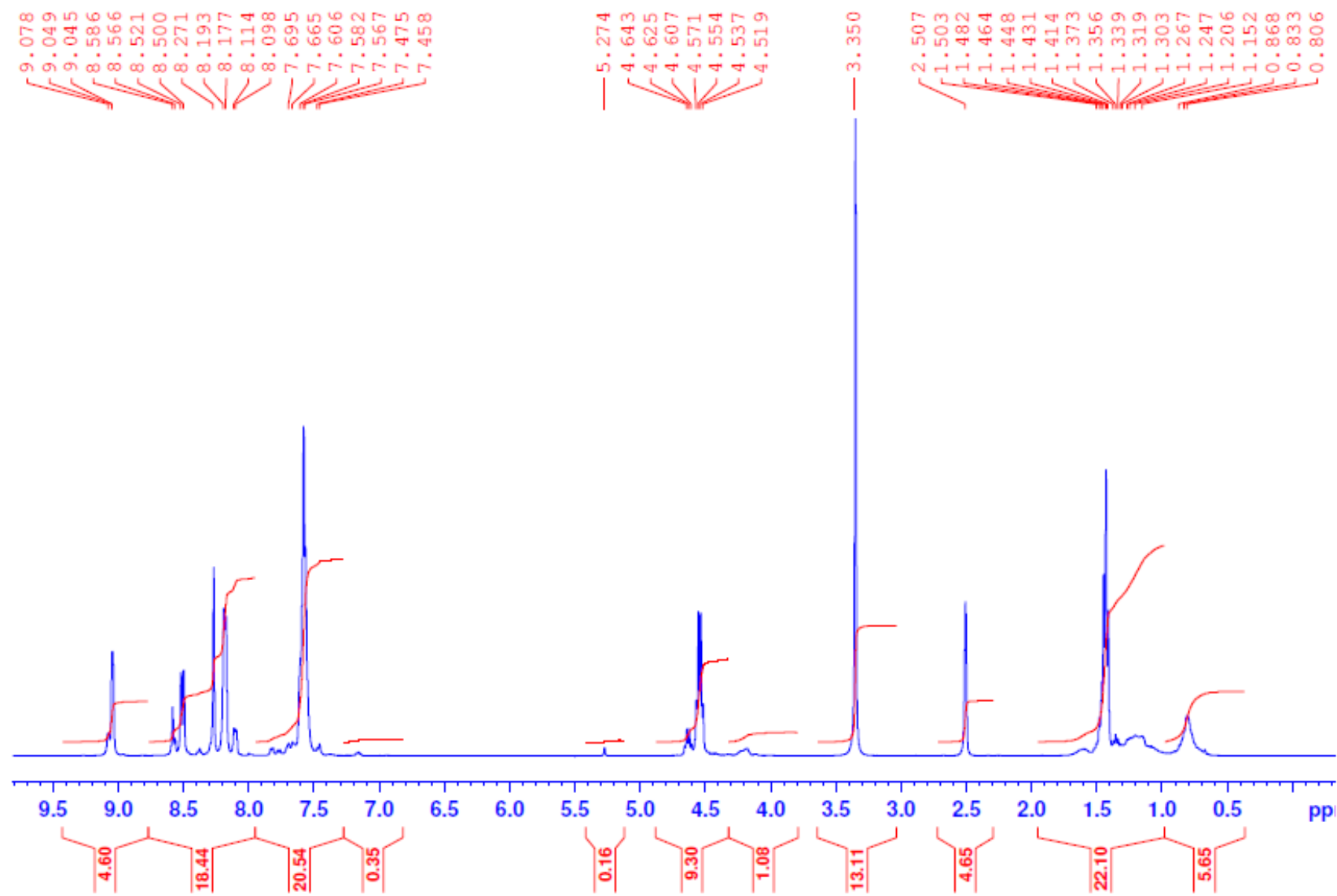
Molecular simulation results offer a molecular rationale for the anti-BVDV activity.

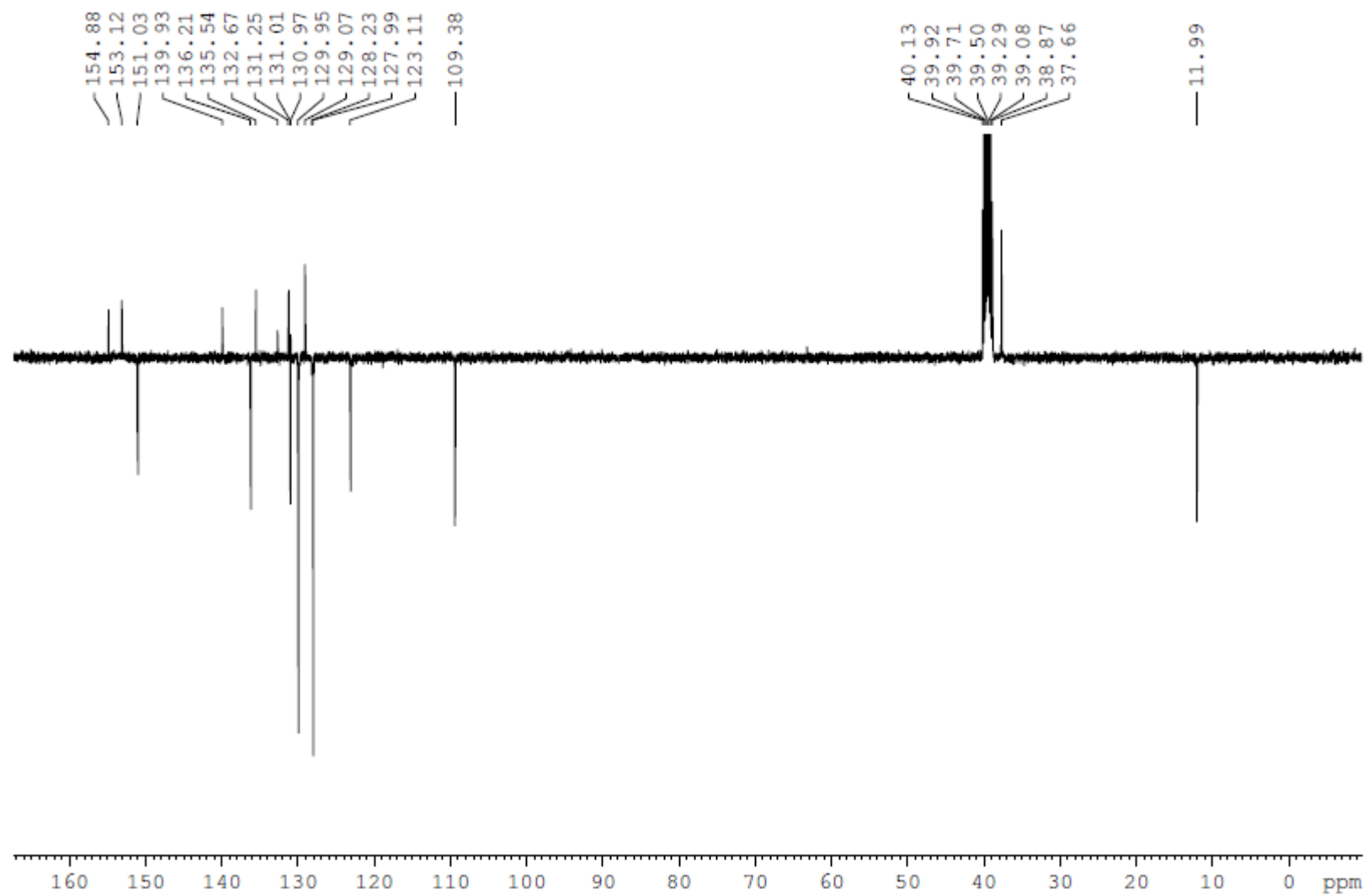
Some compounds were evaluated for their activity on the BVDV RdRp.

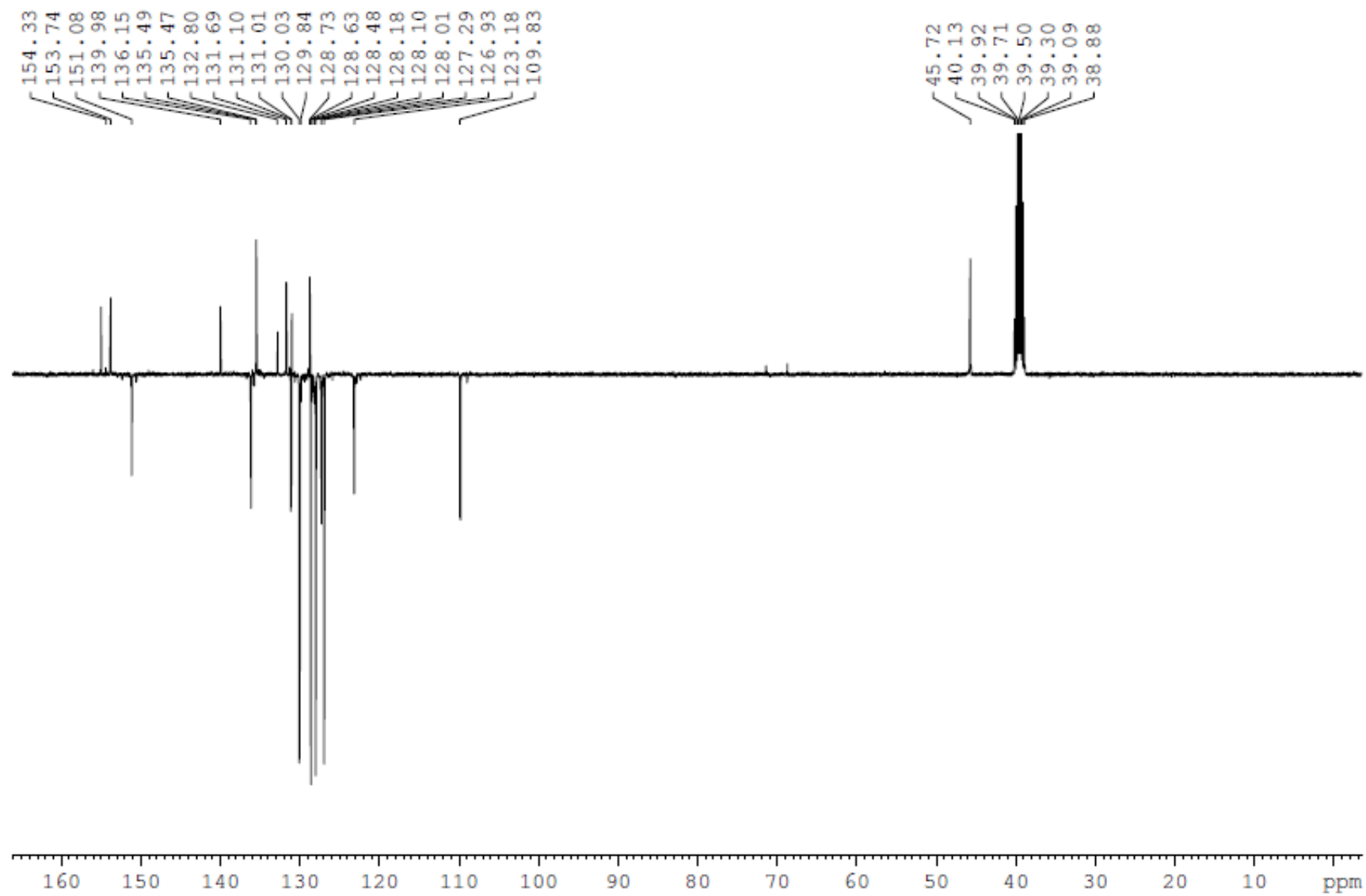
COMPOUND 14B - $^1\text{H-NMR}$ 

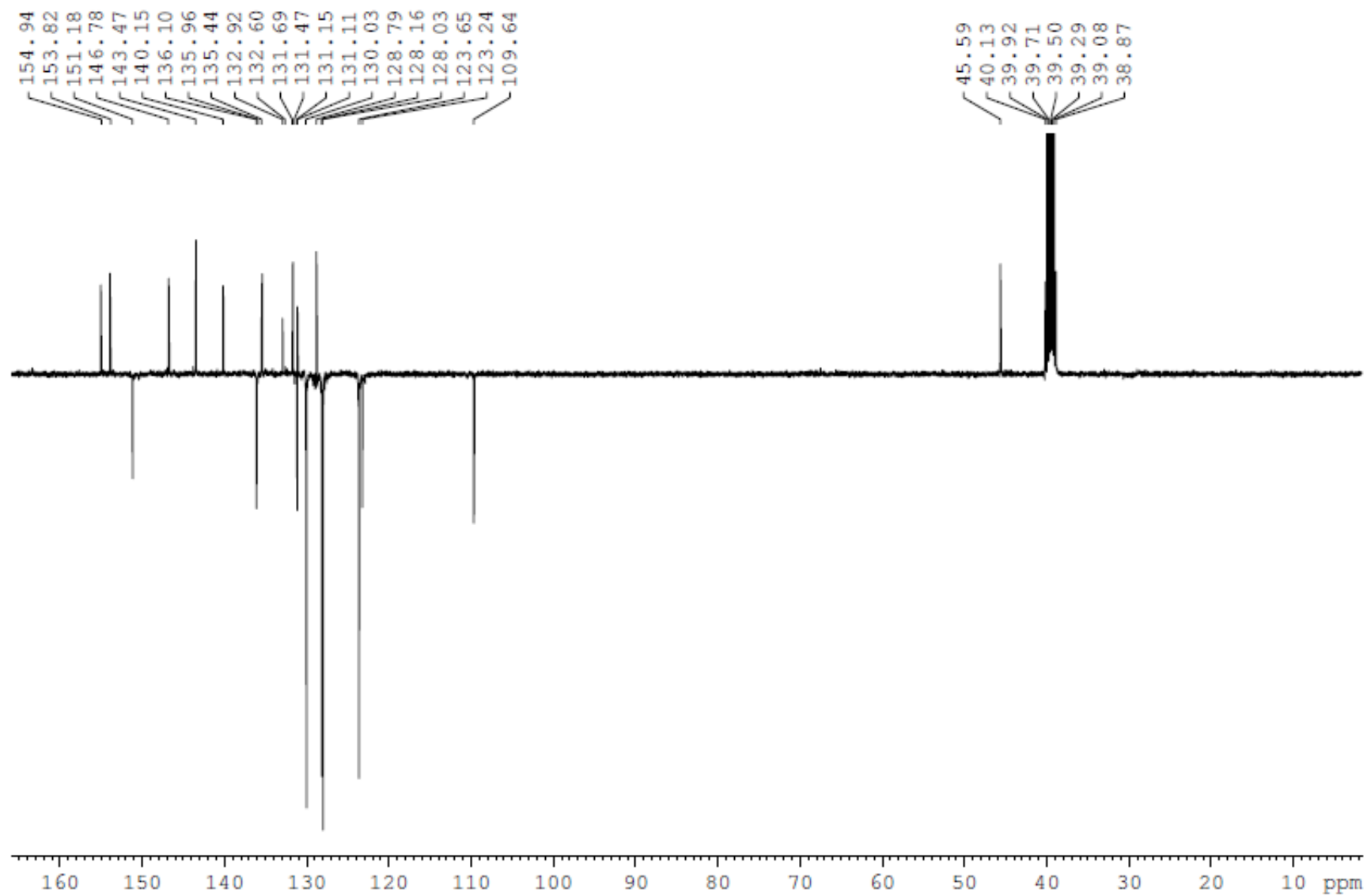
COMPOUND 14D - $^1\text{H-NMR}$ 

COMPOUND 14E - $^1\text{H-NMR}$ 

COMPOUND 15B - $^1\text{H-NMR}$ 

COMPOUND 14B - ^{13}C -NMR

COMPOUND 14D – ^{13}C -NMR

COMPOUND 14E – ^{13}C -NMR

COMPOUND 15B – ^{13}C -NMR